Mapping the extent and change of gully erosion in the Rosendal region, eastern Free State

by

Mtembu Odwa Ntsika (674269)

A thesis submitted to the Faculty of Science, University of the Witwatersrand, Johannesburg, in partial fulfilment of the requirements for the degree of Master of Science (Geography and Climate Change) at the School of Geography, Archaeology & Environmental Studies

Supervisor: Dr Cletah Shoko

Johannesburg, South Africa 2021

Declaration

I declare that ***Mapping the extent and change of gully erosion in the Rosendal region, eastern Free State*** is my own work, that it has not been submitted before for any degree or examination in any other university, and that all the sources I have used or quoted have been indicated and acknowledged as complete references.

Odwa Ntsika Mtembu

Signed

Date: 31 May 2022

ABSTRACT

Understanding the nature and dynamics of gully systems, and how changes in climatic conditions and land use and land cover might influence gully development is crucial for land management and agricultural practices. Studies on land use and land cover changes have frequently been conducted globally with very few covering detailed changes at a local scale and seldomly integrate the influence of extreme rainfall events in the area. Consequently, many areas experience severe gully erosion within a short or very long period of time with minimal response and effective land management practices to sustain their farming land and protect their livestock. Using remote sensing and the Random Forest algorithm, this study analysed the gully development in Rosendal, eastern Free State in South Africa, and changes with other associated land use and land cover changes from 1975 to 2019. The results showed a total increase of 12% in gulled area and 21% increase in bareland area. The overall accuracies of the six (6) classified images, over the study period ranged from 93.95% to 98.17%, with Kappa co-efficients ranging from 92.94% to 97.88%. The study further determined extreme rainfall events and their influence on gully development in the area from 1945 to 2019. The results showed that the years 1993, 2010 to 2011 and 2016 were the top wettest years, and top driest years being 1981 to 1984 and 2015 to 2016. Since 1945, the years 1993, 2005 to 2006, 2010 to 2013 and 2016 had the most extreme rainfall events associated with increased gullied area, with more gully development coupled with intense extreme high rainfall over a shorter rainfall period in 1993. The increased occurrence of intense rainfall over a shorter rainfall period coupled with drier rainfall periods over a longer period potentially influences the increased gully development in the area. Overall, this study shows mapped and quantified dynamics of gully development and the influence of extreme rainfall events on gully development at a local scale over a short and longer period.

Keywords

Agricultural practices, Extreme rainfall events, Extreme rainfall Indices, gully development Image Classification, Land Management, land use and land cover, Remote Sensing.

Acknowledgments

Greatest appreciation and praises are to my Creator and Father: The God Almighty for the strength and healing through all encountered challenges. Camagu kumzi kaPhalo, Abantu Abadala: my ancestors ooNyawuza and the Dlomo clan for their protection and wisdom. Camagu!

This Masters thesis could not have been completed without the love and support from my friends, colleagues and my family who were also my study mates; thank you. To my siblings (Siyabulela and Vuyolwethu), niece (Sibabalwe) and my parents (Mr. O.W. Mtembu and Mrs. C.N Mthembu); thank you for your encouragement, believing in me and forever pushing me to reach greater heights- together we grow; always and forever. I truly appreciate you all and truly lovely you deeply. To my late brother, Snethemba Sthembiso Mtembu, your legacy carries on and thank you for making me believe in achieving the impossible and staying true to myself on issues of education, discrimination, equality and more within my field of practice. You have all played an important role in my academic and professional growth.

Many thanks to the Department of Water and Sanitation especially the Career Management (Ms. Verena Meyer and Ms Nobulali Mtikitiki), Human Resource Development and Surface and Groundwater Information directorates management (Mr. Z. Maswuma, Mr. F. Ramusiya, Mr. T. Mokgatle and Dr. P.L. Mokoena) and team for their support and funding my research.

During my research and writing this thesis, I engaged with a lot of experts, academics, and students in the field and to all of them, I say “thank you. I would like to also show my appreciation to World Merit South Africa, Global network of World Merit and the Wetskills Foundation who also provided their support. encouragement every day and remained very patient with me from day one; I thank you and may the good Lord continue to bless you with all the community and youth development work you are doing in South Africa and globally.

To my supervisor, Dr Cletah Shoko, nothing would have been possible without you. You were a blessing to me, and your guidance gave me strength when I needed it and your patience and understanding enabled healing when times were tough: stay blessed and thank you for everything. To my postgraduate MSc coordinator Dr Mary Evans; I thank you for your support, guidance, and patience. Thank you for availing yourself, believing in this research topic and being present during the hardships encountered during the study. God Bless you all!

Thank you all; may God bless you to provide the same support and more to others to come after me. Together, we can achieve much more in our communities and globally.

Dedication

I dedicate my research work to my late brother, Snethemba Sthembiso Mtembu, who was laid to rest on the 25th of February 2012 a few months before finishing his undergraduate studies at the Walter Sisulu University (WSU) majoring in Mechanical Engineering. Gone, but not forgotten and you will forever be in our hearts and all your hard work for the years God blessed us with you will not be lost in vain. I love and miss you, Brother.

I also dedicate this work to all the learners, students, LGBTQIA+ community and young professionals around the world who continue to fight for gender equality, access to data and information, addressing inequality, hate crime and discrimination in our communities, advocating for radically inclusive learning and working spaces and most importantly, equal quality education for all in all fields of practice. “We are the ones we have been waiting for” and together, we can build a world of meriters beyond political, social, religious and geographical borders. Special dedication to the black queer African community fighting for equal rights and justice for the fallen members of the community to homophobia, Afrophobia, and hate speech even during this current era and democratic government in SA.

Lastly, I dedicate this research work to my parents, Mr. O.W Mtembu and Mrs. C.N Mthembu who both served this country as public servants for more than 30 years as educators in the deep rural areas of Mqanduli in the Eastern Cape Province, South Africa. Your commitment to education and giving back to the community will forever be something I will cherish and advocate for until my very last day on earth as an activist, scientist, social entrepreneur and researcher. You both sacrificed advancing in your professions to allow me, my siblings and generations to come an opportunity to go beyond the limits that were set for you; opportunities for us to be the first of many things you could not have.

For all your love, support, sacrifice and more; I thank you; *Ndiyabulela bazali bam* and this work is for us all and for my grandparents.

Table of Contents

List of Figures

List of Tables

Abbreviations and Acronyms

DEM	Digital Elevation Model
ENVI 5.4	Exelis Visual Information Solutions version 5.4
ESP	Exchangeable Sodium percentage
FLAASH	Fast Line-of-sight Atmospheric Analysis of Hypercubes
GCP	Ground Control Points
GE	Google Earth
GIS	Geographic Information System
KC	Kappa Co-efficient
LDN	Land Degradation Neutrality
LULC	Land Use and Land Cover
LULCC	Land Use and Land Cover Change
MSS	Multispectral Scanner System
NIR	Near Inferred
OA	Overall Accuracy
OBIA	Object based image analysis
OLI	Operational Land Imager
PA	Producer Accuracy
PBIC	Pixel based Image Classification
PCC	Post Classification Comparison
RF	Random Forest
RGB	Red-Green-Blue
RF	Random Forest algorithm
RS	Remote Sensing
S	South
SANSA	South African National Space Agency
SfM	Structure from Motion photogrammetry
SRZ	Summer Rainfall Zone
SWIR	Short-wave infrared
TLS	Terrestrial Laser Scanner
TM	Thematic Mapper
UA	User Accuracy
UAV	Unnamed Aerial Vehicle
UTM	Universal Transverse Mercator
WGS84	World Geodetic System 1984
WRZ	Winter Rainfall Zone

YRZ	Year-round Rainfall Zone

CHAPTER 1: INTRODUCTION

1.1 Introduction

Globally, soil erosion is one of the major environmental concerns. In addition, Africa is currently one of the regions with severe soil erosion, gully development and land degradation (Chase & Meadows, 2007). This continues to have an impact on soil profile, especially fertility, which ultimately affects agricultural practices in many areas. Soil erosion is a natural process caused by wind, ice and water which causes significant land degradation due to loss of soil productivity and quality, and sedimentation of water resources (Ritchie, 2000).

Gully erosion is a severe form of soil erosion by water that involves the removal of soil in channels (gullies) by concentrated runoff either on the surface or subsurface level (Taruvinga, 2008; Liberti et al., 2009; Perez & Garcia, 2017). Gully processes occur when the geomorphic threshold is exceeded, as a result of decreased resistance to erosion, increased erosivity or both (Patton & Schuum, 1975; Perez & Garcia, 2017) causing aggressive removal of topsoil. In some gullied areas, deep incisions on the surface of the area and removal of fertile topsoil are common (Liberti et al., 2009) and these areas are generally not suitable for agricultural activities (Gallart et al., 2002; Taruvinga, 2008; Ferrer et al., 2017). Gully dimensions vary over space and time, ranging from 0.5 to 30 m deep and 80 m wide (Garland et al., 2000; Poesen et al., 2002) due to differences in soil type, slope, and intensity of water activity. For example, in South Africa, some gullies can be 2 km long, 50 m deep and 80 m wide (Garland et al., 2000)

Anthropogenic and natural factors influence the occurrence of soil erosion and gully development. Natural factors, particularly climate (e.g., rainfall) and topography (e.g., soil) and their interaction creates more dynamic and complex erosional process and can further worsen soil erosion in some areas (Chase & Meadows, 2007). For example, changes in rainfall patterns can result to more gully erosion depending on rainfall intensity and duration of the rainfall period. Over the years, changes in climate have caused various short to long term events with more severe impacts experienced in most vulnerable regions such as African regions. Areas that are already vulnerable to erosion and are exposed to more intense rainfall patterns over a shorter rainfall period or drier rainfall periods over a longer period, are more susceptible to soil erosion (Ferrer et al., 2017; Perez & Garcia, 2017; Chase & Meadows, 2007). Climate projections linked to land degradation in Africa highlight a more severely degraded landscape in many African countries (Chase & Meadows, 2007). While gully erosion continues to occur naturally, unsustainable human activities can further result to more gully erosion and more intense impacts of gully development, especially in regions that are vulnerable to gully development (Taruvinga, 2008). For example, overgrazing and deforestation are some of the human activities which expose soil to erosion and gully development. The study by Dube et al. (2017) also highlighted that anthropogenic practices, such as overgrazing and cultivation have resulted to intense land degradation in South Africa. Furthermore, inadequate land management has worsened the conditions as areas become more vulnerable to natural disasters and unsuitable development especially in developing countries (Ferrer et al., 2017; Perez & Garcia, 2017). The monitoring of gullies and their development is a critical step towards sustainable land management and avoiding its impacts on land and livelihoods (Perez & Garcia, 2017).

Different approaches have been implemented to monitor gully developments. To improve monitoring of gully erosion at local to regional scale, many studies (e.g., Taruvinga, 2008; Bernatek-Jakiel et al., 2016; Wilson et al., 2015; Dube et al., 2017; Ferrer et al., 2017) have been conducted by utilizing modern mapping techniques which integrate the use of remotely sensed data. For example, in South Africa, Dube et al. (2017) conducted a study in King Sabata Dalindyebo municipality, in the Eastern Cape Province, on the use of Landsat series data to analyse the spatial and temporal variations of land degradation. To improve monitoring and assessment of the gully systems in the area, Dube et al. (2017) recommended the use of different mapping and monitoring practices when conducting a study on long-term changes to further understand the dynamics and behaviour of the gully systems and land degradation in an area.

1.2 Problem statement

Many studies have been conducted on gully development and mapping at regional scale (Bader, 1962; Berjak et al., 1986; Taruvinga, 2008; Le Roux et al., 2007; Mararakanye & Sumner, 2012; Kuhn, 2013; Bernatek-Jakiel et al., 2016). For example, Taruvinga (2008) mapped gullies in KwaZulu Natal in South Africa, using remote sensing by looking into the utility of three Landsat TM-derived vegetation index techniques and three classification techniques. This was achieved by studying their level of accuracy compared to traditional gully mapping methods applied to SPOT 5 panchromatic imagery at selected scales. The findings of the study showed that the Normalized Difference Vegetation Index produced the highest accuracy for mapping gullies at lower level compared to transformed Soil Adjusted Vegetation Index. Mararakanye and Le Roux (2012) study also produced a location gully map for South Africa where Free State shows gully systems covering 64 674 ha with more gullies in areas close to cultivated land. The study was conducted at a national scale based on visual interpretation and vectorisation of SPOT 5 imagery with acquisition dates varying from 2008 to 2016 at a scale of 1: 10 000. In this regard, the lack of gully mapping at a local scale continues to hinder progress in gully mapping and understanding land use and land cover changes over the years (Ferrer et al., 2017). The spatial heterogeneity at local level further emphasizes the need to focus on these areas to have a better understanding of the occurrence of gullies and their developments. This is difficult to detect at regional scale.

Meadows and Hoffman (2003) further highlighted the significance of mapping gullied areas in South Africa at local scale to understand their expansion and contraction which is crucial for decision making processes (Perez & Garcia, 2017). Le Roux and Sumner (2012) also argued that a detailed gully mapping study at local level will further enable identification of currently vegetated or gully-free areas susceptible to continuous gullies and discontinuous gullies development in areas highly vulnerable to gully development. Understanding mapped gully systems at local level, especially in South Africa, will further improve our understanding of the importance of gully controlling factors from a field to catchment perspective to allow scale-specific management intervention. The development of classification algorithms such as Random Forest and rainfall indices for determination of extreme events also provide deeper and more detailed insights to the mapped landscape patterns and identified rainfall patterns.

In addition, the influence of extreme rainfall events on the development of gullies, remain unclear. Extreme rainfall events play an important role in the development of gullies due to their rainfall intensity and influence on erosion over a longer or shorter period (Han et al., 2017). Bocco (1991) and Conforti et al. (2011) further emphasized the importance of understanding the influence of climate on erosional processes for better understanding of land use and land cover changes during the mapping process. It is therefore important to provide knowledge on integration of climate data analysis, by determining extreme climate events and changes in rainfall patterns over a long period to better understand gully development.

1.3 Aims and Objectives

The aim of this study was to determine the spatial and temporal development of gullies from 1975 to 2019, as well as to assess the influence of extreme rainfall events on gully development, in the Rosendal area of the eastern Free State, South Africa,

This was achieved through the following specific objectives:

- To map gullies and other associated land use and land cover changes in Rosendal using multi temporal Landsat data at ten-year intervals.

- To quantify the dynamics of gully development from 1975 to 2019.
- To assess the influence of extreme rainfall conditions on gully development from 1975 to 2019.

1.4 Thesis structure

This thesis is divided into five different chapters. **Chapter 1** is the general Introduction, which provides a brief introduction to the study, aim, specific objectives, problem statement and thesis structure. **Chapter 2** provides a review of literature, highlighting the theoretical background to this study, relevant scientific literature on gully development and mapping techniques in South Africa and beyond. In **Chapter 3,** techniques and methods followed to achieve the specific objectives of this study are outlined, including the background of the study area, data collection, processing, and analysis. **Chapter 4** reports the major findings of the study. **Chapter 5** provides discussion of the possible explanations to the findings and relating findings to previous studies. Finally, **Chapter 6** concludes the main findings of the study, limitations encountered and provides recommendations for further studies.

CHAPTER 2: LITERATURE REVIEW

2.1 Overview of Land degradation

Land degradation is one of the environmental challenges globally. Approximately 10% of the world's land surface has been degraded by erosion (Nacinovic et al., 2014) and gully erosion severely contributes to the acceleration of land degradation. Land degradation is the loss in natural resources (soil, water, flora, and fauna) or biophysical processes by which it functions (Abdi et.al., 2013) as a result of complex inter-relationships between biophysical and socio-economic issues. It involves reduction in the abundance and composition of vegetation and negative changes in the physical, biological, and chemical properties of the soil (Abdi et al., 2013). For example, land degradation decreases soil productivity and quality as it reduces organic matter and removes fine grained particles during erosion. Land degradation results in the destruction of the ecosystem (such as generation of clean surface water) and loss of crops (affecting agricultural activities) due to decreased soil fertility (Rosenberg, 2011). Consequently, rural disadvantaged areas suffer the most due to their high dependence on land for agricultural practices (Kuhn, 2013). This is a significant environmental problem in Africa, especially in sub-Saharan Africa and South Africa (Department of Environmental Affairs, 2012) as many areas practice farming (domestic and commercial).

The causes of land degradation are very complex and not entirely distinct as they can be due to anthropogenic practices and climatic factors, such as drought and overgrazing (Meadows & Hoffman, 2003). Over the years, many areas in arid, semi-arid and dry sub-humid regions have been exposed to severe land degradation characteristic of desertification due to climatic variations and human activities (Abdi et al., 2013). Rapid global population growth has caused increased demand for good quality, affordable and sustainable goods, and services for all. This increased demand has led to increased economic and infrastructural development, especially in developing regions. The increase in infrastructural development has placed an increasing pressure on environmental sustainability due to unsustainable anthropogenic practices (Perez & Garcia, 2017), especially during colonization (Meadows, 2003). The unsustainable anthropogenic practices continue to negatively impact the state of the landscape. For example, in South Africa, Kakembo and Rowntree (2003) have highlighted a strong spatial correlation between abandoned cultivated land and gully erosion, and these are typically highly degraded areas with historical unsustainable land management (Taruvinga, 2008; Kuhn, 2013).

As the demand for global land resources is increasing with development across different sectors, production of these resources is declining. To better manage this crisis, the land degradation neutrality (LDN) aims at maintaining or enhancing land-based natural capital and its associated ecosystem services (Cowie et al., 2018). The United Nations Convention to Combat Desertification (UNCCD) has led the development of the Scientific Conceptual Framework for LDN to provide scientific approach to planning, implementation and monitoring of the land degradation neutrality (Akhtar-Schuster et al., 2017; Cowie et al., 2018). Actions and strategies developed to accomplish the LDN include sustainable land management practices to avoid or reduce degradation, combined with efforts to reverse degradation through restoration or rehabilitation of degraded land (Cowie et al., 2018; von Maltitz et al., 2019). Thus, articulating the priorities in planning LDN interventions of the response hierarchy of Avoid > Reduce > Reverse land degradation (Akhtar-Schuster et al., 2017; Cowie et al., 2018).

Von Maltitz et al. (2019) discusses experiences from the South African land degradation neutrality target setting process during the 2017/18 financial year in response to the United Nations Convention to Combatting Desertification's call for signatory countries to voluntarily commit to land degradation neutrality as also requested under the Sustainable Development Goal target 15.3. The study concluded that invasive flora and woody plant densification were the most persistent degradation problems needing intervention. This target setting process has resulted to ambitious set of goals being set for 2030, and the use of GIS models and RS approaches can provide better insights for identifying and mapping ecosystem service hotspots for targeting LDN investments in south-eastern Africa (Willemen et al., 2018).

The extent to which the soil continues to be degraded depends on its geological and geomorphological features, and to some extent its protective surface attributes, such as the type and percentage of vegetation cover (Nacinovic et al., 2014). Areas with little to no vegetation cover are more vulnerable to land degradation as bareland is highly susceptible to any form of erosion (Kuhn, 2013).

2.2 Understanding the relationship between LULCC and gully development

Understanding and defining the concept of land use and land cover change (LULCC) has been changing and developing over the years due the complex dynamics and nature of geomorphological processes. Lambin et al. (2003), and Ozsahin et al. (2018) define land cover as the observed biophysical cover on the earth's surface which is inclusive of built-up area, grassland, forest, and cultivation. Land use composes of traits by activities and practices conducted by people on a certain land cover for specific needs and wants (domestic and commercial) (Briassoulis, 2000); these can include, not limited to, production and change of maintenance of the land use. Therefore, land use and land cover (LULC) are the distinct characteristic layers of the Earth's surface that can also be closely linked in nature (Stolbovoi, 2002; Meadows & Hoffman, 2003). Land cover provides conditions on the natural and human induced practices on the environment, whilst land use provides additional integrated information on social, economic, and natural factors on the environment. LULCC can be quantified to changes in the aerial extent of a certain area where there might be an observed decrease or increase in LULC (Stolbovoi, 2002).

Various LULC classes exist and were previously grouped into broad classes such as, forests, grassland, water bodies, agricultural land, and built-up area (Taruvinga, 2008). Over the years, these LULC classes have been redefined to accommodate more anthropogenic practices influencing the observed environmental changes and responses from nature per region. As literature and research developed over the years, LULC classes have been inclusive of bare land and gullied areas due to increased land degradation in many regions and their noticeable contribution to land degradation (Ozsahin et al., 2018). As a result of the different activities over time affecting LULC, LULCC can be grouped into two categories namely conversion and modification. Conversion refers to changes from one use or cover type to another whilst modification refers to maintenance of the general land use of cover change (Stolbovoi, 2002; Ozsahin et al., 2018).

Gullied areas are crucial land cover areas during LULC classification for understanding gully development or mapping of gullies in a certain area. Changes in anthropogenic practices, population growth and increased soil erosion results to more erosional processes and increased observed LULCC in an area (Ozsahin et al., 2018) which makes it important for researchers to determine more relevant classification classes fit for their study especially in areas exposed to severe soil erosion and gully erosion. Gullied areas are dynamic and complex severely eroded areas due to gradual erosion over a longer period (Kuhn, 2013). These gullied areas differ in sizes and characteristics due to differences in internal and external factors controlling and influencing gully development (Kuhn, 2013; Bernatek-Jakiel & Poesen, 2018). As a result of their nature to develop over a longer period, changes in climatic conditions and increased unsustainable human activity in an area can result to accelerated gully erosion (Kuhn, 2013). In more vulnerable areas, accelerated gully erosion can also include severe resultant features such as pipping and closed depressions that develop over a shorter period (Bernatek-Jakiel & Poesen, 2018).

2.3 Gully development and types of gullies

There are two types of gully development processes due to distinct erosion processes which can result to continuous gullies and discontinuous gullies (Le Roux & Sumner, 2012).

Comparing these two types of gullies, Le Roux and Sumner (2012) concluded that continuous gullies develop due to various factors such as gentle footslopes, erodible soils derived from mudstones and overgrazing which causes poor vegetation cover. In comparison, discontinuous gullies mostly occur on hillslopes, relatively stable and shallow soils. In areas where overgrazing is coupled with susceptible mudstones, detailed mapping and analysis of the gullies is crucial as these are significant factors to consistently determining development of continuous gullies and discontinuous gullies (Le Roux & Sumner, 2012; Yibeltal et al. 2019).

Boardman et al. (2015) highlight a 13-year record of erosion in the Karoo area in South Africa and further provides some insight on gully systems within the area. Sites in this area have been exposed to intense overgrazing for a very long time (Boardman et al., 2015). From the study by Boardman et al. (2015), it was established that most of the gully systems tend to develop in the valleys (major and tributary) of Sneeuberg. Gully formation in the Karoo can be dated back to between 1820 and 1850 (Bordman et.al., 2015) as the observed gullies are a response to environmental changes dating back to European settlement (Rowntree, 2013). The study further concluded that understanding gully systems at a local or regional scale also requires being aware that some gully systems pre-date human induced impacts on the environment, although most recently developed gully systems may be a result of overgrazing and soil piping in some areas, (Bernatek-Jakiel & Poesen, 2018).

Piping is the formation of linear voids (pipes) by concentrated flowing water in soils, unconsolidated or poorly consolidated sediments (Jones, 2004; Bernatek-Jakiel & Poesen, 2018). Soil piping increases the erodibility and susceptibility of a surface as it exposes the roots from the roof of a pipe. Intense rainfall over a short period of time or normal rainfall over a long period of time can easily detach vegetation through erosion by water as the roots will be exposed from the bottom. Although piping is mostly an erosional process driven by water erosional process, it can also be as a result of mass movements processes (Bernatek-Jakiel & Poesen, 2018). Piping is a complex process that occurs in different landforms such as plains, hills and valleys (natural landforms) and in agricultural terraces, cities and road drainage systems (anthropogenic environments) (Bernatek-Jakiel & Poesen, 2018). Due to the dynamics and complexity of piping erosion at subsurface, controlling and detecting soil pipes for land management purposes remains a hindrance towards achieving sustainable development in affected areas as soil pipes remain invisible at the surface until the pipe roof collapses (Bernatek-Jakiel & Poesen, 2018). At the soil surface, closed depressions, sinkholes and discontinuous (blind) gullies are indicators of pipe collapses (Figure 1) which form pipe inlets, pipe outlets, pipe fan and pipe mounds (piping-related features) (Bernatek-Jakiel & Poesen, 2018).

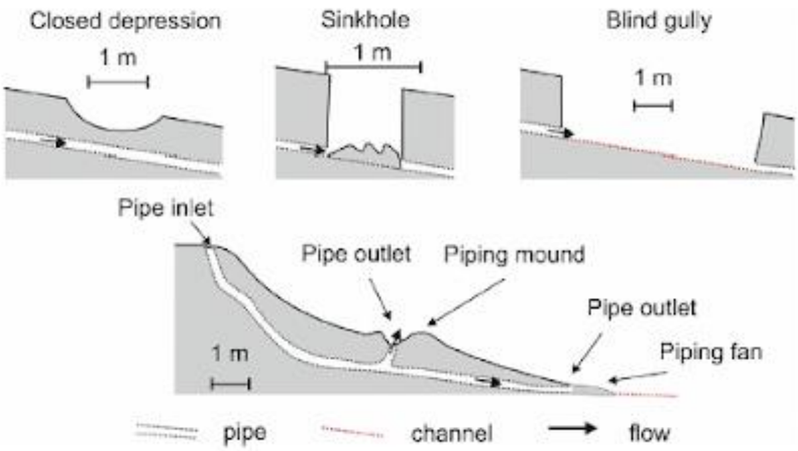

Figure 1: Piping forms and piping-related features

Closed depressions develop as a result of the soil surface lowering slightly above a pipe without causing any break in the vegetation cover (Bernatek-Jakiel & Poesen, 2018). Overtime, these features develop to sinkholes as the soil surface gets exposed to more erosion and eventually collapses creating nearly vertical walls. Ultimately, occurrence of more erosional processes and disruption within piping systems results to more soil collapses forming sinkholes, and these sinkholes eventually develop to discontinuous gullies as a result of the sequential soil collapses or enlargement of a sinkhole due to a roof collapse of a pipe (Bernatek-Jakiel & Poesen, 2018). Continuous piping on the gully channel causes newer gully development, widening of the existing gully channels and accumulation of sediment on the gully floor. In addition to erosional forms such as pipe collapses, soil piping also results to depositional forms such as piping fans and sediment mounds. Bernatek-Jakiel and Poesen (2018) describe piping fans as a result of sediments being transported by water without being restricted by pipe walls (after the sediments pass through the pipe outlet) and are eventually deposited as fan due to decreased transportation capacity and flow rate. Sediment mounds are typically formed around a pipe outlet as a result of sediment being deposited on grass – covered soil surfaces on gentle slopes (Bernatek-Jakiel & Poesen, 2018).

Gully pipes consist of vertical headcuts (shallow to deep) and hollow soil pipes (pipe formation) beneath the surface, which form as a result of fine particles being washed out along distinct sub-surface layers within the soil (Sumner & Meiklejohn, 2000). Garcia-Ruiz et al. (2013) and Ferrer et al. (2017) further describe piping as a process that is characteristic of abundant expansive clays, dispersive soils, strong gully incision due to hydraulic gradient and soil erosion processes with a less permeable layer at depth. Dispersive soils are derived from various rock types (such as sedimentary rocks of the Beaufort Group, Dwyka Group and Ecca Group; Karoo Supergroup) and can be found mostly in drier areas (Bell & Maud, 1994; Bell & Walker, 2000). Dispersive soils have no threshold velocity for erosion thus making them very susceptible to erosion and piping (Bell & Walker, 2000). Easy dispersion is as a result of presence of exchangeable sodium (ESP) percentage and the higher the ESP, the more prone the soil is to dispersion as dispersed particles move into surrounding pores (Chen & Bordochovich, 1983; Bell & Walker, 2000) and also have a higher potential for soil piping.

Very often, gullied areas are associated with piping and very steep gully walls. Garcia-Ruiz et al. (2013) and Ferrer et al. (2017) further describe piping as a process that is characteristic of abundant expansive clays, strong gully incision as a result of extensive hydraulic gradient and associated with a less permeable layer at depth. Piping processes have been identified as crucial for understanding gully development (Garcia-Ruiz et al., 2013), as they remain a huge controlling factor for gully processes (Valentin et al., 2005; Calvo-Cases et al., 2011). Areas exposed to gully erosion have become one of the most crucial geomorphic areas (especially in Mediterranean regions) due to their high erodibility, low vegetation cover, heavy rainfall, and steep topography (Garcia-Ruiz et al., 2013), and their high erosion rates make them an ideal study area to conduct multiscale mapping techniques (Gallart et al., 2013; Ferrer et al., 2017). To better manage gullied areas, understanding their expansion or contraction is a crucial factor to be considered for mapping purposes and decision-making processes (Meadows & Hoffman, 2003; Valentin et al., 2005; Perez & Garcia, 2017).

2.4 Internal and External factors controlling gully erosion

The rate, severity, and distribution of gully systems in an area is greatly dependent on several internal and external factors controlling and influencing gully erosion (Jahantigh & Pessarakli, 2011). These internal factors (such as topography, bedrock, and soil type) and external factors (such as climate, and human activities) are responsible for controlling the nature and development of the erosional systems, especially gullies (Botha, 1996; Ferrer et al., 2017; Perez & Garcia, 2017). Topography is an important factor that determines erosion potential as it controls the energy gradients (Taruvinga, 2008; Conforti, 2011). Topographical features control erosion due to the slope gradient, length, and shape (earthen floodplains of river valleys are more prone to erosion than rocky flood channels) (Morgan, 1986; Ferrer et al., 2017). In addition, soil type controls the nature in which a gully system develops as soil property determines porosity, fertility and susceptibility of the topsoil exposed to soil erosion (Perez & Garcia, 2017; Yibeltal et al. 2019). Yibeltal et al. (2019) highlighted the morphological characteristics and topographic thresholds of gullies in different agro-ecological environments in northwest Ethiopia. The study characterized 94 gullies for 10 morphological parameters in three environments and concluded that gully length is the most dynamic parameter in all agro-ecologies. Berjak et al. (1986) highlight that gully erosion in South Africa mostly occurs in areas characteristic of shale, whilst Bader (1962) associates South African gullies with areas underlain by dolerite. Taruvinga (2008) linked South African gullies to areas of minimal to no vegetation cover (bareland) and unconsolidated topsoil.

It is often easy for researchers to classify gullies based on process either being surface or subsurface erosional processes. Surface erosion involves displacement of soil particles by impact of raindrops, whereas subsurface erosion involves movement of fine soil particles within the soil which eventually leads to pipe formation beneath the surface (Sumner & Meiklejohn, 2000). It is important to note that these systems are: 1) a product of many integrated processes that change the landscape and 2) develop over a short to long period of time depending on various internal and external factors influencing or controlling the system (Le Roux et al., 2007). Whilst topography and soil type are one of the key factors controlling and influencing gully erosion, climate influences the rate at which gully erosion occurs in a short or longer period due to the changes in rainfall intensity, frequency and occurrence over a certain period of time (Haylock & Nicholls, 2000).

Over time, various studies have thoroughly highlighted the increased negative impact caused by human activities such as overgrazing, overstocking of livestock, deforestation, and infrastructural development (Lal, 2001; Taruvinga, 2008; Kuhn, 2013; Perez & Garcia, 2017). For example, Perez and Garcia (2017) conducted a study in southeast Madrid (Spain) to monitor soil erosion in a recently urbanized area built on clastic sediments and soils. The study showed that the evolution of soil erosion varied across the area depending on anthropic influences and vegetation cover. Furthermore, findings of the study also argued that recent urbanization increased the erosion of sandy materials in the area. Many South African soils have been exposed to extensive poor land management due to overgrazing, infrastructural developments, wildfires, and deforestation leading to severe surface and subsurface erosion (Taruvinga, 2008). Land use changes only trigger the underlying soil profile to re-equilibrate and adapt to the current ecosystem’s condition without preserving or recovering the original properties of the paleosol (structure, nutrients and water carrying capacity), (Valentin et al., 2005). Consequently, despite various attempts to reduce or limit anthropogenic practices on degraded land through conservation measures; vegetation cover recovery and soil cover recovery might not occur simultaneously at the same rate (Bands 1985; Kuhn 2013; Perez & Garcia, 2017).

Despite various studies (Montgomery, 2007; Taruvinga, 2008; Vanwellghem et al., 2017) having emphasized the significance of sustainable land use and management, lack of synchronized and integrated policies to protect the environment, inclusive of monitoring and evaluation measures, remains a serious management issue (Meadows & Hoffman, 2003). A more detailed and better understanding of the soil process (especially in areas with increased urbanization or significant vegetation loss) is very useful for land use planning (Perez & Garcia, 2017). Land management policies, implementation strategies, programs and projects that address physical environmental practices need to be considerate of the geomorphological processes in the area, especially the dynamics related to the underlying strata and geohydrological processes in systems such as gullies.

2.5 Climatic influence on soil erosion and gully development

Climate has the potential to directly influence the rate of gully erosion through rainfall (frequency and intensity), temperature and vegetation cover (indirect influence) (Moore 1979; Kuhn, 2013). Climate controls the conditions in which the vegetation grows (Taruvinga, 2008; Kuhn, 2013) and rainfall is the main factor that is associated with erosional processes (Moore, 1979; Kuhn, 2013). A series of studies (Capra et al., 2008; Nachtergaele et al., 2001; Han et al., 2017) have reported that extreme rainfall events promoted gully development due to high rainfall intensity and changes in rainfall duration and occurrence. For example, Han et al. (2017) reported accelerated gully development (especially in agricultural fields) in Fuxian County (China) during periods of high rainfall intensity, frequency and short durations which exceeded the rainfall characteristic threshold. The findings of the study by Han et al. (2017) were achieved through studying the effects of rainfall regime and variability on soil loss with gully erosion based on a twelve (12) year record in Fuxian County, Shaanxi Province of China. Capra et al. (2008) conducted a study in Raddusa (Italy) and outlined the relationship between rainfall characteristics and gully erosion from 1995 to 2007. This study showed the influence rainfall has on gully erosion in the area through analysis of rainfall index to account for the most severe erosive events which also corresponded to the more wet rainfall period October to January annually.

Temperature is one of the important climatic factors affecting soil erosion especially in mid latitude areas (Wu et al., 2018). Changes in temperature directly control the freeze-thaw process, especially in areas exposed to extreme temperatures and high erosivity (Li & Fan, 2014). The freeze-thaw process controlled by temperature changes impacts soil erosion due to its influence on soil aggregate stability. While low temperatures coupled with average to higher rainfall may lead to more soil erosion in freeze-thaw areas (Li & Fan, 2014), Onwuka and Mang (2018) reported that an increase in temperature increases soil erosion rate as soil temperature results to changes in radiant energy and energy changes occurring through the soil surface. It therefore controls the physiochemical and biological processes inclusive of gas exchange between the soil and the atmosphere which are responsible for the amount of heat supplied to the soil surface and dissipated from the soil surface down the profile. Understanding the changes in soil temperature is crucial for understanding erodibility influenced by the rate at which organic matter decomposes and mineralization (Onwuka & Mang, 2018)

Changes in temperature further impact the soil moisture and water availability which directly control vegetation growth. Areas with high vegetation cover are less vulnerable to erosion due to the stability and fertility of the soil profile (Kuhn, 2013). Little to no vegetation cover exposes the soil surface to any kind of erosion with more erosivity experienced in areas with unconsolidated soil or bareland (Taruvinga, 2008). Consequently, areas with high rainfall over a longer rainfall period (or higher rainfall intensity over a shorter period of time) are highly vulnerable to erosion. The impact of soil erosion is more intensive in areas with little to no vegetation cover and high rainfall (Taruvinga, 2008; Kuhn, 2013). It is the intensity of rainfall, soil erodibility and other surface conditions that directly determine the amount of soil to be detached from the surface or moved within the subsurface (Van Dijik et al., 2002; Ferrer et al., 2017). In addition to this, the type of vegetation in the area is controlled by the intensity of erosion in an area, however, this all depends on rainfall frequency and intensity (van der Eyck et al., 1969; Conforti et al., 2011).

2.5.1 Extreme rainfall events and their impact on gully development

Understanding rainfall frequency and intensity requires analysis of trends in rainfall over a long period. Through a study conducted in Australia for a period of 1910 to 1998, Haylock and Nicholls (2000) discuss the three crucial rainfall indices and methods for understanding extreme events namely: *extreme frequency, extreme intensity, and extreme percent*. *Extreme Frequency*- this rainfall index determines the number of events above the extreme threshold (long-term 95thpercentile) (Haylock & Nicholls, 2000). Outcome values are crucial to examine changes in the number of extreme events by counting the number of events in a year with intensities above rainfall threshold; the threshold can be calculated by determining the mean 95th percentile. *Extreme Intensity*- this index determines the average intensity of rainfall (rain falling in the highest events) from extreme events (Haylock & Nicholls, 2000). Outcome values can be used to describe changes in the upper percentiles and changes in all events above the upper percentile. *Extreme percent*- this index determines the proportion of the total rainfall (rainfall falling in the highest events) from extreme events (Haylock & Nicholls, 2000). Outcome values of this index can be used to determine changes in the upper portion of the daily rainfall distribution. Any observed changes in the percentage of the total rainfall from the higher events can provide an indication of changes in the shape of the rainfall distribution, which is useful for the extreme percent index. In addition to understanding the different extreme indices, analysis of changes in rainy days is key to understanding short to long term seasonality changes.

A study conducted by Xu et al. (2017) focused on the impact of both topography and rainfall indices on gully erosion in China (Loess Plateau). The study reported a strong and direct influence of rainfall pattern on gully erosion through analysis of rainfall intensity as the main rainfall index. It was also concluded that soil loss was higher when rainfall intensity increased and much higher where high rainfall intensity corresponded to increased slope and upslope drainage. In South Africa, although the use of rainfall indices has not been fully analysed to determine extreme events, a study by Nel and Sumner (2007) determined rainfall intensity to understand and determine the most extreme erosive rainstorms in Drakensberg from late 2001 to late 2006. The study concluded that the most extreme rainstorms with higher rainfall intensity occurred almost exclusively in summer resulting to more erosion. The study further noted the significance of understanding the seasonal changes or shifts in rainfall periods as the rainfall events in KwaZulu Natal Drakensberg also showed the significant variation in rainfall duration with some highly erosive extreme rainfall events occurring in a short period of time during the drier winter season. Areas with little to no vegetation cover and exposed to extreme rainfall events are highly susceptible to soil erosion (Kuhn, 2013), and arid and semi-arid regions are prone to gully erosion (Xu et al., 2017).

2.6 Gully erosion mapping and monitoring techniques

Mapping in the pre-digital era was achieved using various methods and tools such as the plane table, varying combinations of measuring tapes, manual theodolites, compass, and levelling aids (Gillespie, 1875; Almeida-Warren et al, 2021). Spatial mapping using these techniques has limitations and constraints such as; they are time consuming, sensitive to movement and often require frequent readjustment of the tools (Almeida-Warren et al, 2021). All these limitations result to higher chances of inaccurate measurements with the tape and compass being the least reliable and most prone to random human and instrument error (Almeida-Warren et al, 2021). While some of these methods are still in use, there has been great development in mapping and monitoring methods and techniques to improve accuracy, speed, and automation of these methods.

There are gully mapping and monitoring techniques that depend on field observation data and there are techniques based on remote sensing and Geographic Information Systems (GIS) application. Traditional mapping methods for gullies include digitization of the outer boundary of the gully banks from an aerial photo or satellite image or both (Taruvinga, 2008). In many cases, groundtruthing and stereographic viewing using air photographs has been crucial for minimizing challenges encountered with vegetation cover causing challenges on marking the outline of the gullies (Taruvinga, 2008). Nachtergaele and Poesen (1999) conducted a study in central Belgium assessing soil losses by gully erosion using high altitude aerial photographs. The study mapped gullies covering 218 ha which formed over a three-year period. The gullies were simultaneously measured and mapped both in the field and by high altitude aerial photos. The study further showed that using both these mapping methods ensured better results compared to if one method was used which would have only detected and mapped 75% of the gullies.

Since various developments and improvements in GIS and Remote Sensing (Kivel, 1991; Sohl & Sleeter, 2012; Yengoh, 2016), mapping land use and land cover change has advanced especially with historical changes in landscape. As a result of this, various studies have been conducted globally using airborne and spaceborne mapping techniques to understand and analyse LULC and gully development (Lambin & Geist, 2006). Satellite image data is crucial in gully mapping as it can provide land cover information at more frequent interval compared to information provided by traditional techniques. This has made it possible to have satellite remote sensing data available as regional datasets produced at more regular intervals, like SPOT and Landsat medium resolution datasets, as well as low resolutions datasets such as Moderate Resolution Imaging Spectroradiometer (Ellis, 2013). High spatial resolution sensors can provide detailed gully attributes but they are not freely accessible, especially for large areas and long temporal coverage. Low spatial resolution for MODIS datasets has resulted to lack of intensive studies in mapping and monitoring gully development (Seutloali et al., 2015). Landsat 8 is one the recent images with a better (higher) spatial resolution of the Landsat series which has made it more effective to conduct classification of LULC due to its Operational Land Imager sensor and Thermal Infrared Sensor responsible for improved noise performance (USGS, 2014). Le Roux (2012) produced a gully location map for South Africa using visual interpretation and vectorisation from SPOT 5 imagery at a scale of 1:10 000 using GIS. The study succeeded in providing results showing the spatial extent of gullies in South Africa at national level. Results further indicated that 4.3% of gullies mostly occurred in areas suitable for cultivation compared to the 1.5% of land not suitable for cultivation. Despite challenges and limitations experienced during the mapping and interpretation process due to similarity of classing causing difficulty in distinguishing gullies from riverbeds, the overall accuracy was 90% when compared to observations.

There are different types of air-bone remote sensing techniques namely, Terrestrial Laser Scanner (TLS), terrestrial Structure from Motion Photogrammetry (SfM) and aerial SfM photogrammetry with an Unmanned Aerial Vehicle (UAV, that is, drones) used globally to better understand and map soil erosion, especially gully erosion in highly vulnerable and degraded areas. This type of remote sensing mapping technique is very well advanced at high spatial resolution but very expensive. Table 1 summarizes the strengths and weakness of these different remote sensing techniques based on their resolution of the point clouds and the scale at which a study is conducted.

Table 1: Strengths and weaknesses of the different techniques, (Ferrer et al., 2017). All techniques are non-invasive.

Technique	Strengths	Weaknesses
TLS	• High Data acquisition • Fast post-processing • High accuracy potential and automation level	• Costly (monetary and time) • Heavy material • Issues with little misalignments of reference points
SfM	• Low weight and low costs • Covers larger ground of the study area (minimal data missing) • Data collection is faster	• Centimetric accuracy • Post-processing is time consuming • Not good for surveying very large areas
UAV	• Easy useful in inaccessible areas • Good for data collection in medium to large study areas	• Time consuming post Processing and license requirements • Issues with data capturing from vertical and complex surfaces • Centimeter range accuracy

The study by Ferrer et al. (2017) in the Ebro Depression in Spain discuss the use of these multiscale approaches to assess geomorphological processes in semiarid gullied areas. The findings of the study showed few recorded topographical changes from data obtained with TLS due to topographic shadows in comparison to terrestrial SfM. The study concluded that

TLS is crucial for fast processing of data and has huge potential for data acquisition, SfM photogrammetry allows 3D models to be created from multiple overlapping images taken at distinct triangulation angles and UAVs are ideal for medium to large study areas, inaccessible areas and good for understanding gully system dynamics (inclusive of piping mapping) at larger scales. Bouchnak et al. (2009) further conducted a study at Draix observatory in France where the findings of the study concluded that the use of drones to generate high-accuracy Digital Elevation Models (DEMs) and mapping products in systems like gullies has provided valuable results for soil erosion.

Seutloali et al. (2015) further discussed the significance of the use of robust mapping measures, such as remote sensing (RS) and GIS, to better understand the contribution of roads to soil loss in the south-eastern region of South Africa. The study used vegetation cover, rainfall and gradient of the discharge hillslope integrated with remotely sensed data (Landsat dataset) and GIS to determine whether these factors could provide insight to gully morphology in the area. The study concluded that rainfall and vegetation cover have minimal influence on gully morphology and argued for a detailed gully mapping using modern techniques such as UAV in relation to rainfall and vegetation cover for gully systems that are not along roadsides.

One of the main limitations of RS in LULC detection and mapping gullies is its inability of some sensors to collect data in some areas for seasonal analysis due to presence of cloud cover (Liberti et al., 2009; Yengoh, 2016). In addition to that, confusion in analysing LULCC may occur as a result of similarity of minimal contrasting classification of some areas. Furthermore, when mapping gullies in areas also prone to soil piping, detecting, and mapping soil pipes in the gully systems is one of the biggest challenges due to the presence of both vertical and horizontal soil pipes at sub-surface (Bernatek-Jakiel & Poesen, 2018). Use of drones to map soil pipes only provides location of the pipe roof collapses, pipe inlets and pipe outlets at the soil surface; thus, excluding mapping of the horizontal soil pipes present within the piping system. In addition to that, mapping of gullies at local scale is costly and time consuming (Ferrer et al., 2017) due to the need for long-term studies to verify the suitability of different traditional and modern mapping techniques in areas with complex landscape and issues associated with quantifying topographical changes or erosion rates (Ferrer et al., 2017).

Integration of climate or anthropogenic factors in modelling and mapping of gully development has improved over the years, due to increased interest and studies on the influence of climate on gully development at a regional scale. However, only few studies have been conducted on the influence of climate on gully development at local scale. This has caused hindrance on ensuring sustainable land use and management, especially in developing countries. For example, Bands (1985) conducted a study in Groot Winterhoek Wilderness Area in the

Western Cape Province of South Africa using RS and GIS on the influence of mountain catchment area control measures on land management focusing on ecological, economic, and social implications. The findings of the study showed that the mapped gullied area from early industrialization to 1985 covering 0.015% of the area was caused by domestic stock (80%), demand for access to routes (19%) and cultivation (01%). Bands (1985) further argued that the gully systems were still unstable in some parts of the area due to accelerated gully erosion associated with unsatisfactory land management. Kuhn (2013) also conducted a study in Groot Winterhoek Wilderness Area in the Western Cape Province of South Africa. The study used remote sending and GIS on long-term vegetation change and the influence anthropic practices have on LULCC especially on vegetated and gullied areas. The findings concluded that areas exposed to intense grazing, and frequent and intense wildfires had experienced more gully erosion. Kuhn (2013) further concluded that lack of vegetation in some parts of the area increased vulnerability to more soil erosion during extreme rainfall periods. However, since the protection of the area by local authorities, some gullies were stabilizing, and this change was brought due to the changes in land management from intense overgrazing by farmers to highly protected conservation area which allowed for increase in vegetation cover and prohibited grazing.

Lu et al. (2018) further demonstrated the direct relationship between gully development and rainfall through the application of Google Earth (GE) images and ASTER GDEM as means of exploring the feasibility of open data source in large-scale gully mapping in the Loess Plateau (China). The mapping results of the study proved the approach efficient for extracting gully affected areas with an overall accuracy of 78.80% despite the complexity of the gully network in the area. Through the use of object-based analysis (OBIA) and pixel-based image classification (PBIC) methods, Karami et al. (2015) conducted gully mapping in Lamerd (Iran). The accuracy comparison findings of this study showed that OBIA produced better classification than PBC due to the improved textural and shape features of OBIA. However, the use of standard feature space and reduction of the salt-pepper effect by OBIA limited the observed features on the output maps of gullies compared to PBC.

CHAPTER 3: MATERIALS AND METHODS

3.1 Study Area

Rosendal is a town in Free State Province of South Africa (28.50°S, 27.93°E) with an area of approximately 8.5 square kilometres. The study area itself is located south of Rosendal (Figure 2) in the eastern region of Free state province.

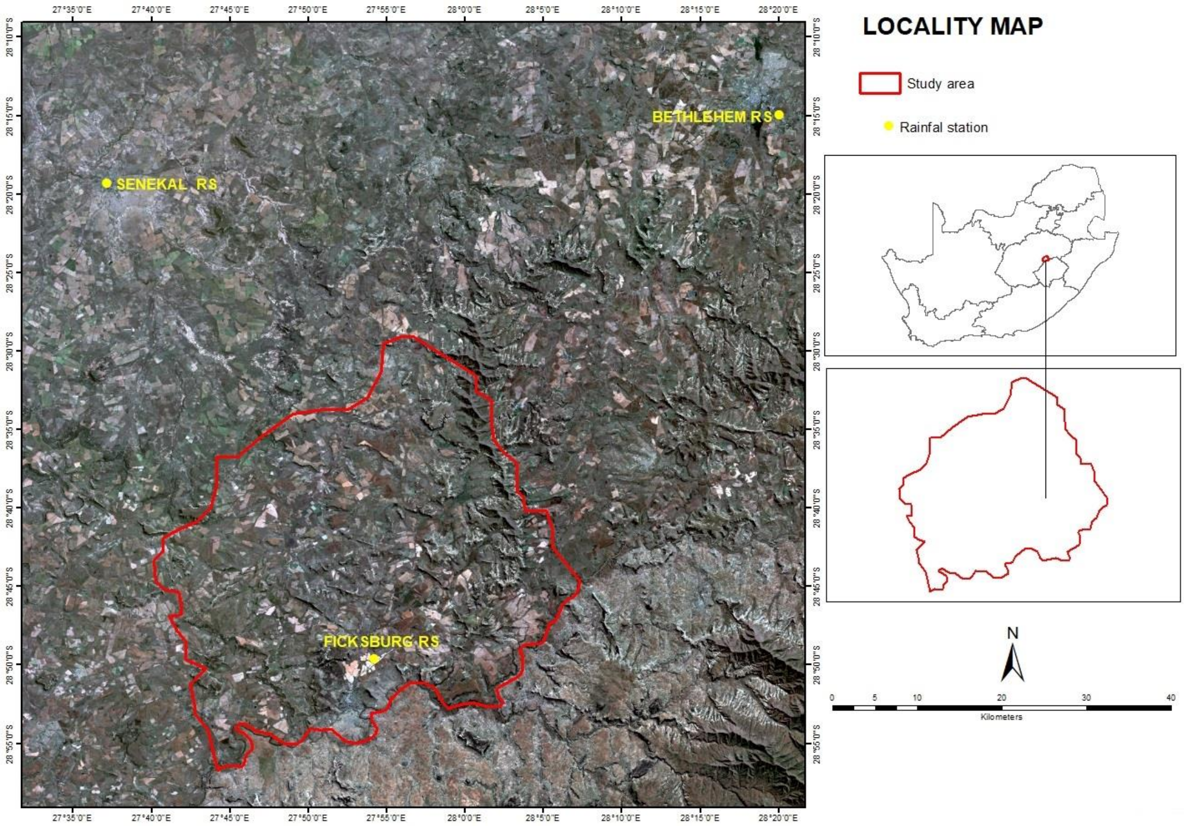

Figure 2: Satellite image showing the study area in the Free State Province, South Africa. *(Image: SPOT6 for 2015. Bands: RGB-543)*

3.1.1 Geology

Rosendal geology consists of the Dwyka and Ecca Group (older group) overlain by the Beaufort Group and Molteno, Elliot and Clarens Formations (younger rocks) (Brandl et al., 2006). All these rock types are capable of having dispersive soil which are highly susceptible to erosion and soil piping (Bell & Walker, 2000). The study area is covered by the Beaufort Group (lower Adelaide and upper Tarkastad subgroup) which is characteristic of mudstone and sandstone with a greater abundance of both sandstone and mudstone in the younger Tarkastad Subgroup (Brandl et al., 2006). The underlying geology of the study area is dominated by alternating sand and clay layers (intercalated arenaceous and argillaceous strata) mapped in Figure 3, which is principally argillaceous strata and porous unconsolidated and consolidated sedimentary strata of the Beaufort Group (Brandl et al., 2006).

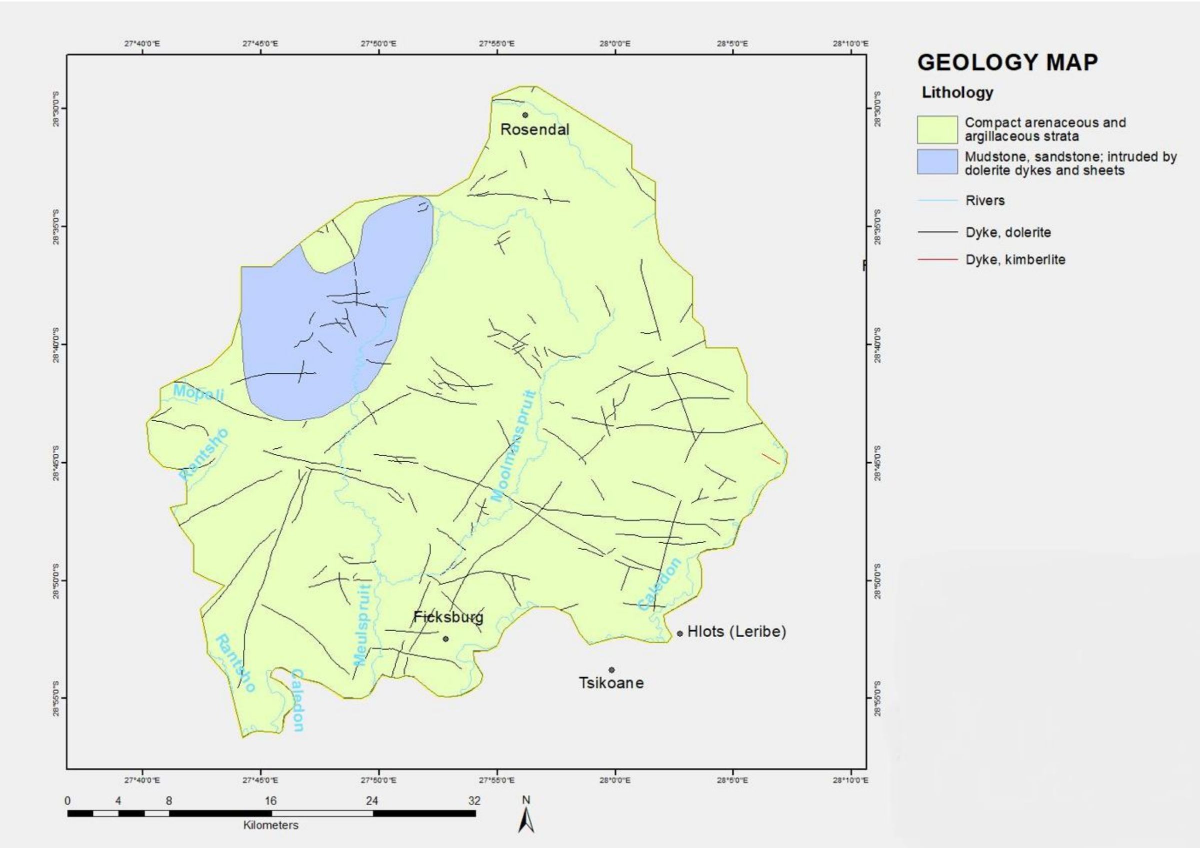

Figure 3: Map showing the geology of the study area. (*Data Source: DWS, SA)*

The study area is made up of soils derived from the siliciclastic rocks with compact arenaceous and argillaceous strata, and mudstones and sandstones intruded by dykes, sheets and dolerites (Figure 3). These are dispersive and high erodible soils due to their high vulnerability to erosion. The average terrain elevation above sea level is 1 400 m with rugged topography characteristic of moderate to steep ridges and gentle slopes near farms and valley floors.

3.1.2 Climate

According to Chase and Meadows (2007), the Free State Province falls within the summer rainfall zone (SRZ) where Rosendal receives mid-summer rainfall of about 600 mm to 700 mm annually with average maximum temperatures of 30°C in summer (January is the hottest month) and average minimum temperature of 11°C in winter (June is the coldest month). The SRZ is characteristic of heavy summer seasonal rainfall (December to February), and very cold and dry winter seasons (June to August) (Chase & Meadows, 2007). Autumn (March to May) and spring (September to November) are also characteristic of rainfall in some parts of

South Africa such as the Rosendal area in eastern Free State region (Chase & Meadows, 2007; Kuhn, 2013).

3.2 Data acquisition

3.2.1 Remote sensing data acquisition

Landsat images (six sets) covering the study area were obtained from the Department of Water and Sanitation with support from South African National Space Agency (SANSA). The Landsat imagery in Tables 2 (a and b) per decade (as per study objectives) were used for this research and the different band wavelengths per dataset. The selected Landsat satellite images dates were influenced by: 1) the quality of the image, especially for those with limited or low cloud cover, 2) rainfall season (Spring to autumn: September to May) and 3) period of ten years as per study objective. The preferred months are November to March but due to cloud cover and low temporal resolution of Landsat data, some images are outside this preferred period. For example, there were no clear images available for TM for the preferred months to maintain consistency hence images for October and September were used.

Table 2: Different Landsat imagery datasets and band wavelengths used for the study

a) Landsat imagery dataset used per decade and spatial resolutions

Landsat dataset	**Number of bands**	**Spatial resolution (m)**	**Acquisition date**
MSS	4	60	03 December 1975
TM	7	30	05 March 1985, 11 October 1995 20 September 2005
OLI	8	30	05 December 2015 14 November 2019

Note: MSS= Multispectral Scanner System, TM=Thematic Mapper and OLI= Operational Land Imager

b) Band wavelengths for the different Landsat datasets used

MSS Landsat dataset			TM Landsat Dataset			OLI Landsat Dataset		
Band	Description	Wavelength (μm)	**Band**	Description	Wavelength (μm)	**Band**	Description	Wavelength (μm)
4	Green	0.5 – 0.6	**1**	Blue	0.45 – 0.52	**1**	Coastal aerosol	0.43 – 0.45
5	Red	0.6 – 0.7	**2**	Green	0.52 – 0.60	**2**	Blue	0.45 – 0.51
6	NIR	0.7 – 0.8	**3**	Red	0.63 – 0.69	**3**	Green	0.53 – 0.59
7	NIR	0.8 – 1.1	**4**	NIR	0.76 – 0.90	**4**	Red	0.64 – 0.67
			5	SWIR	1.55 – 1.75	**5**	NIR	0.85 – 0.88
			6	Thermal Infrared	10.40 – 12.50	**6**	SWIR 1	1.57 – 1.65
			7	SWIR	2.08 – 2.35	**7**	SWIR 2	2.11 – 2.29
						9	Cirrus	1.36 – 1.38

3.2.1.1 Reference data collection

Rwanga and Ndambuki (2017) discuss that reference data is important to show and build the relationship between surface features and localities by validating and standardising remote sensing imagery. This is applicable to both field data and observations about regions or objects that are remotely sensed. Google Earth (GE) images were used as reference source and training samples were obtained for mapping the land use classification and validation. GE is an important spatial data source that has been used to extract information for different land use and land cover types (Bagan & Yamagata, 2012). Training samples were collected for the images of 1975, 1985, 1995, 2005, 2015 and 2019 and were digitised on GE. The training samples ranged from 300 to 500 samples for each of the eight classes for this study: ridge (310), Built Up (300), Dense vegetation (335), gully (432), Water body (364), Cultivated land (500), bareland (480) and sparse vegetation (429). The following Land Use/Land Cover (LULC) classes were used in the study:

- Ridge: narrow and very long mountain hilltops.
- Built Up: residential and commercial areas covered with buildings and houses in the urban areas, periphery and rural areas.
- Dense vegetation areas covered with trees (forest) and shrubs
- Gully: deeply incised and steep-sided erosional surfaces.
- Water Body: Lakes, reservoirs, streams, rivers, swamps.
- Cultivated land: land surfaces covered with crops.
- Bareland: land surfaces with exposed soil, rocks or sand.
- Sparse vegetation: areas covered with grassland and bushes

It proved difficult to digitise Landsat TM as the images were blurry while Landsat OLI/TIRS were crystal clear but all images were used during data processing. Furthermore, this sampling dataset was utilised for the accuracy assessment of the classification. The dataset was processed using the R-Studio software and was separated into 70% training data and 30% testing data for validation. This division ensures accuracy estimates that are 1) valid (do not overestimate the accuracy or underestimate the approximation error) and 2) more accurate among the valid estimates (overestimation of the approximation error is the smallest possible) (Gholamy et al., 2018).

3.2.2 Rainfall data acquisition

Daily total rainfall data from 1945 to 2019 was received from the South African Weather Service National Climate Centre. Data received was for Senekal, Bethlehem and Ficksburg which are the three areas proximal to Rosendal, with rainfall stations. The data were as follows:

- Senekal: daily total rainfall data from 1945 to 2019.
- Bethlehem: daily total rainfall data from 1993 to 2019.
- Ficksburg: daily total rainfall data from 1977 to 2019.

The three stations have different data record as outlined above: Senekal (74 years), Bethlehem (42 years) and Ficksburg (26 years). These three towns were chosen for this study because Rosendal has no rainfall station, and these three towns are the closest towns with reliable rainfall stations. Senekal, Bethlehem and Ficksburg are 41 km (Northwest), 81.3 km (Northeast) and 45 km (South, near South Africa and Lesotho border) away from Rosendal, respectively.

3.3 Data processing

3.3.1 Remote sensing data preprocessing

Pre-processing of images is crucial as remotely sensed imagery is often distorted due to various external factors such as atmospheric conditions, topography and seasonal variations, (Rwanga & Ndambuki, 2017). All images were pre-processed using the Exelis Visual Information Solutions (ENVI 5.4) software where atmospheric correction, including radiometric correction, was conducted and applied through the Fast Line-of-sight Atmospheric Analysis of Hypercubes (FLAASH) tool. Each Landsat was georeferenced and orthorectified to Universal Transverse Mercator Zone 35 South (UTM Zone 35 S) projection based on the World Geodetic Datum (WGS 84) coordinate system. To account for the difference in spatial resolution of the images, (60 m for MSS and 30 m for all other images), Nearest Neighbour resampling method was applied to allow all images to be analysed at the same spatial resolution of 30 m. Nearest Neighbour resampling was the most appropriate method to use because it is an efficient method in which each pixel in the resampled raster acquires the same value as its nearest neighbour in the original raster (Lu & Weng, 2005).

3.3.1.1 Image classification

All images were classified using the Random Forest (RF) classification method through the R-Studio software. Random Forest classification is the most relevant classifier to use due to its high flexibility and ease of implementation. It uses randomness to enhance its accuracy and combat overfitting (Rwanga & Ndambuki, 2017)

Band combination is crucial for determination of landscape features due to different frequencies of the electromagnetic spectrum which are separated into different bands (Rwanga & Ndambuki, 2017). An appropriate spectral band combination was selected during the image classification based on the objectives of this study to effectively distinguish between vegetation (healthy and unhealthy), urban area, water, and soil. For Landsat imagery 8, red-green-blue (RGB)-543 band combination for vegetation and RGB-432 were used to distinguish the different LULC classes used in this study. For other Landsat images (Landsat 5 and Landsat 2), band combinations RGB-431 and band combination RGB-542 were used during image classification. The selected band combination was firmly concluded effective by Taruvinga (2008) during a gully mapping using remote sensing study in KwaZulu Natal, South Africa. The RGB-432 band combination shows images in a natural colour composite showing healthy (green) and unhealthy vegetation (brown), and urban features as white (or grey) and water as dark blue. The band combination RGB-543 makes it easier for the user to process the images as it provides near infrared composite which is useful for more analysis of vegetation to show area with better vegetation health (red), water and urban areas.

3.3.2 Rainfall data processing

All received data from the three rainfall stations was sorted based on seasons of the defined rainfall period, where the wet season (late spring to mid-autumn) is September to April and the dry season (late autumn and winter) is May to August (Chase & Meadows, 2007; Kuhn 2013). In both seasons, analysis to determine anomalies, changes in rainy days and extreme rainfall events were conducted per decade. To analyse short-term and long-term changes in monthly and annual rainfall in the area, analysis was done for every decade per station. To further check the strength of the data and how the monthly and annual rainfall averages all three stations relate; analysis for 1993 to 2019 period (where all rainfall data record overlap) was conducted.

3.3.2.1 Identification of rainfall period

This study continuously refers to “rainfall period” which is defined as a period with rainy days between September and April where more than 1 mm of rainfall fall was received at any given day and not more than 15 consecutive days passed without any rainfall. This rainfall period was determined and defined as described and argued by Haylock and Nicholls (2000), and chosen by sorting the data, checking any missing data where applicable and plotting monthly rainfall per area throughout the available rainfall data record to identity the months where more than 20 mm per monthly average (per rainfall station) has been received to better fit the purpose of this study. May to August total daily rainfall data was also analysed to check shifts and changes in rainy days and amount of rainfall received during the drier period. Where applicable, some extreme rainfall events occurred either at the beginning or ending of this drier period and these rainfall shifts are crucial for changes in seasonality in this study.

3.4 Data analysis

3.4.1 Remote data analysis

3.4.1.1 Accuracy assessment

Accuracy assessment was conducted on ArcGIS to validate the classified maps. This process aims is to quantitatively assess how effectively the pixels were sampled into the correct land cover classes during the classification, (Rwanga & Ndambuki, 2017). The confusion matrix measures Overall Accuracy (OA), User's Accuracy (UA), Producer's Accuracy (PA) and the Kappa Coefficient (KC), and these are widely used accuracy metrics in LULCC using remote sensing (Guerschman et al., 2003; Pontius & Millones, 2011; Rwanga & Ndambuki, 2017). The OA or total Accuracy provides basic overall accuracy information by summing the correctly classified pixels and dividing them by the total number of reference pixels and is calculated using this formula the formula below:

$$\text{Overall Accuracy (OA)} = \frac{\Sigma \text{ (classes correctly classified)}}{\Sigma \text{ (Row total or column total)}}$$

The Producer Accuracy (PA) refers to the pixels that were omitted from the correct class in the land cover classification map, thus calculating the false negative from the omitted errors (Foody, 2002; Rwanga & Ndambuki, 2017). It is the number of correctly identified pixels divided by the total number of pixels in each class by the number of reference pixels and is calculated using the formula below:

$$\text{Producer Accuracy (PA)} = \frac{\text{Number of correctly classified classes in a column}}{\text{Total of Verified items in that column}}$$

The User Accuracy (UA) represents the percentage of pixels that were anticipated to be in a particular class but were not part of that class, thus calculating the false positives (Thapa & Murayama, 2009; Rwanga & Ndambuki, 2107). UA is calculated using the following formula:

$$\text{User Accuracy (OA)} = \frac{\text{number of correctly classified items in a row}}{\text{Total number of verified items in that row}}$$

The Kappa co-efficient (KC) analysis is a distinct multivariate technique used in accuracy assessment to yield a Khat statistic (estimate of Kappa) to assess the accuracy (or agreement) of a classified thematic map, (Rwanga & Ndambuki, 2017). This Khat statistic is computed as:

$$\kappa = \frac{N \sum_{i=1}^{n} m_{i,i} - \sum_{i=1}^{n} (G_i \, C_i)}{N^2 - \sum_{i=1}^{n} (G_i \, C_i)}$$

where;

i represents the class number,

N is the total number of the pixels classified that are being compared to ground truth dots,

mi, i represents the pixels that belong to the ground class ***i***, that have also been classified with a class ***i***

Ci represents the number in total of classified pixels that belong to class ***i***

Gi represents the number in total of ground truth pixels that belong to class ***i***

Kappa co-efficient ranges from -1 to 1 and a Kappa co-efficient value equal to 1 represents a perfect agreement (assessment accuracy) which is better than random (positive value) or worse than random (negative value), while a Kappa co-efficient value close to zero represents an agreement (assessment accuracy) that is no better than random classification.

3.4.1.2 Change detection to assess changes in gullies

For this study, ENVI 5.4 was used during the change detection process to produce a well detailed table of changes between the six (6) classified images over the decades from 1975 to 2019. These changes have been presented in pixel count, percentages, and area (hectares) as means of quantifying the LULC changes and gullied areas in the area. In remote sensing, change detection is a digital process that captures spatial change from imagery due to natural or manmade occurrences and is very crucial for determination and monitoring of environmental change especially LULC, (Taruvinga, 2008; Rwanga & Ndambuki, 2017). Alsalman et.al (2010) state that many studies have been conducted on the application of Post Classification Comparison (PCC) as the main approach used in remote sensing for determining and monitoring LULC as it detects and provides the most accurate LULC changes compared to other approaches such as image differencing.

3.4.2 Rainfall data analysis

3.4.2.1 Rainfall anomalies and changes in rainy days

By identifying the wettest and driest periods and months in the area since 1945, together with the changes in rainy days and shifts in rainfall period; extreme changes in gully development and extreme events can be understood better. This is achieved by determining the period with *highest* rainfall received (wettest) with a *reduced* (shorter) or *increased* (longer) rainfall period (and total number of rainy days) or vice versa to account for periods that might have accelerated or triggered the observed changes in gully systems. The *more positive* the rainfall anomaly value, the *drier* it was during that season, and the *more negative* the rainfall anomaly value, the *wetter* it was during that season.

To determine the top three driest and top three wettest summer seasons in the area from 1945 to 2019, the following steps adopted from Kuhn (2013) were taken during the rainfall data analysis:

- Calculate Total summer rainfall per summer season of the rainfall period.
- Determine the Mean rainfall-climatology by taking an average of the annual summer season total rainfall received per rainfall period.
- Calculate the anomalies (how wetter or drier it was that particular season) by subtracting the annual summer rainfall received from the Rainfall Climatology to determine the top three driest seasons and top three wettest seasons per rainfall period.

Results obtained from the calculations above were used to account for the observed changes (rejuvenation or expansion) in gully erosion during that season of a particular year using Landsat images, where applicable.

Rainy days were analysed per rainfall station to determine changes in total number of rainy days and shifts in number of rainy days per rainfall period. Rainy day is any day per year during the rainfall period where more than 1 mm of rainfall has been recorded on that day (Haylock & Nicholls, 2000). To strengthen the rainy days data for reliability, no more than 15 consecutive days within the rainfall period can have missing data or rainfall received less than 1 mm (Haylock & Nicholls, 2000). Trend analysis of the changes in rainy days was conducted per rainfall station and compared for the period of 1993 to 2019 were all data sets overlap across all three stations.

3.4.2.2 Rainfall indices to determine extreme events

Understanding and determining extreme indices for long term rainfall data is crucial to better understand the occurrence and changes in occurrence of extreme rainfall events in an area (Haylock & Nicholls, 2000). Three indices were calculated for this study to analyse occurrence and changes in extreme rainfall events in the area: *extreme frequency, extreme intensity, and extreme percent* as proposed by Haylock and Nicholls (2000).

Extreme Frequency determines the changes in the number of extreme events by determining the number of events above the extreme threshold; that is, long-term 95th percentile. *Extreme*

Intensity determines the average intensity of rainfall from extreme events. *Extreme percent* determines the proportion of the total rainfall from extreme events. Following calculation of extreme indices methodology by Haylock and Nicholls (2000), all indices were analysed, and three methods were used to calculate the extreme intensity and extreme percent to account for significant trends in the number of raindays in the area. Raindays are defined as days with at least 1mm of rainfall. Calculations conducted for each year for the three indices are outlined below:

1. *Extreme Frequency*- rainfall threshold per area was calculated by determining the mean 95^{th} percentile for each area. Number of events above the 95^{th} percentile were identified, and outcome values were used to examine changes in the number of extreme events by counting the number of events in a year with intensities above rainfall threshold.
2. *Extreme Intensity*- to determine the average intensity of rainfall per area, changes in the upper percentiles and changes in all events above the upper percentile were analysed by following the calculation steps below:
    a. Calculate an average of the highest four events each year.
    b. Calculate average of the highest 5% of daily rainfall total above 1 mm.
    c. Averaging all events above the long-term 95^{th} percentile.
3. *Extreme percent*- to determine the proportion of the total rainfall from extreme events, changes in the upper portion of the daily rainfall distribution was analysed. Any observed changes in the percentage of the total rainfall from the higher events provided an indication of changes in rainfall distribution, which is useful for the extreme percent index. For each year, the above steps followed to calculate the extreme intensity index were repeated and then;
    a. Divide the extreme intensity by the year's total rainfall per rainfall station.

Total rainfall was analysed together with the extreme frequency and extreme intensity across all areas to determine any possibility of extreme events that are more frequent and intense during certain periods of high rainfall. Such analysis enables better understanding of any observed changes in expanded gully systems in the study area in relation to extreme rainfall.

CHAPTER 4: RESULTS

4.1 Mapping and analysis of LULC changes using multi temporal Landsat data of ten-year intervals.

4.1.1 Image classification and quantification of gully development and expansion per decade using change detection techniques

Figure 4 (a and b) and Figure 5 show the LULCC in the region which was mapped out using the Random Forest (RF) algorithm and Landsat images, at a 10-year interval. Overall, there was a change in gully development and other associated LULC in the region over the 44 years with a clear change in magnitude of gully development, and to some extent, the direction of their growth where clearly visible. Over the years, the gullied and bareland areas have expanded, with a noticeable increase in housing development whilst vegetation cover decreased significantly.

In 1975, as shown in Figure 4 (a and b) gullies are more observed in the northern and southwestern parts and built-up area in the northern and southern parts. Cultivated land is observed in most parts of the region especially the central area. Ridges are dominant on the eastern part of the region whilst sparse vegetation and bareland are mostly observed south-east, central and northwestern parts of the region (Figure 4a).

In 1985, it can be observed that gullied area increased by 5.48% while bareland has increased by 9.08% compared to the previous decade. More gullied area is observed in the western and central parts of the area. Increased bareland is also observed in the area, especially in the central to northern part and southwestern parts (Figure 4a). Sparse vegetation decreased by 16.66% and is more spread out across the central part of the area compared to previous decade where it was a bit more concentrated on the southern part of the area.

In 1995, more changes in gully development and bareland are observed in the area with more gully systems mapped in areas with decreased sparse vegetation. Increased bareland was observed in the southwestern and central parts of the area (Figure 4a). Statistics also confirm that gullied area increased by 4% from previous decade, bareland increased by 6%. On the other hand, cultivated land increased by 2% and built up area increased by 1%, while dense vegetation cover decreased by 1% and sparse vegetation cover decreased by 11%.

In 2005, more gullies are observed in areas mosty dominated by bareland and sparse vegetation. More gullies observed in parts of the area with increased bareland cover and decreased sparse vegetation (Figure 4b). Built-up area continues to gradually increase in the southern and northern parts of the area.

In 2015, more gullies observed in the southern, central and nothern parts of the area(Figure 4b) especially in areas dominated by increased bareland area and derceased dense vegetatation. Increased sparse vegetation is observed in areas dominated by gullies and bareland areas in the central area of the region.

In 2019, compared to the last decade, gullied area, bareland and sparse vegetation dominates the region with some built up area observed in the southern and southeastern parts of the area (Figure 4b). Gullied area increased by 1%, bareland cover and built up area increased by 3% each whilst sparse vegetation and cultivated land decreased by 7% and 1% respectively.

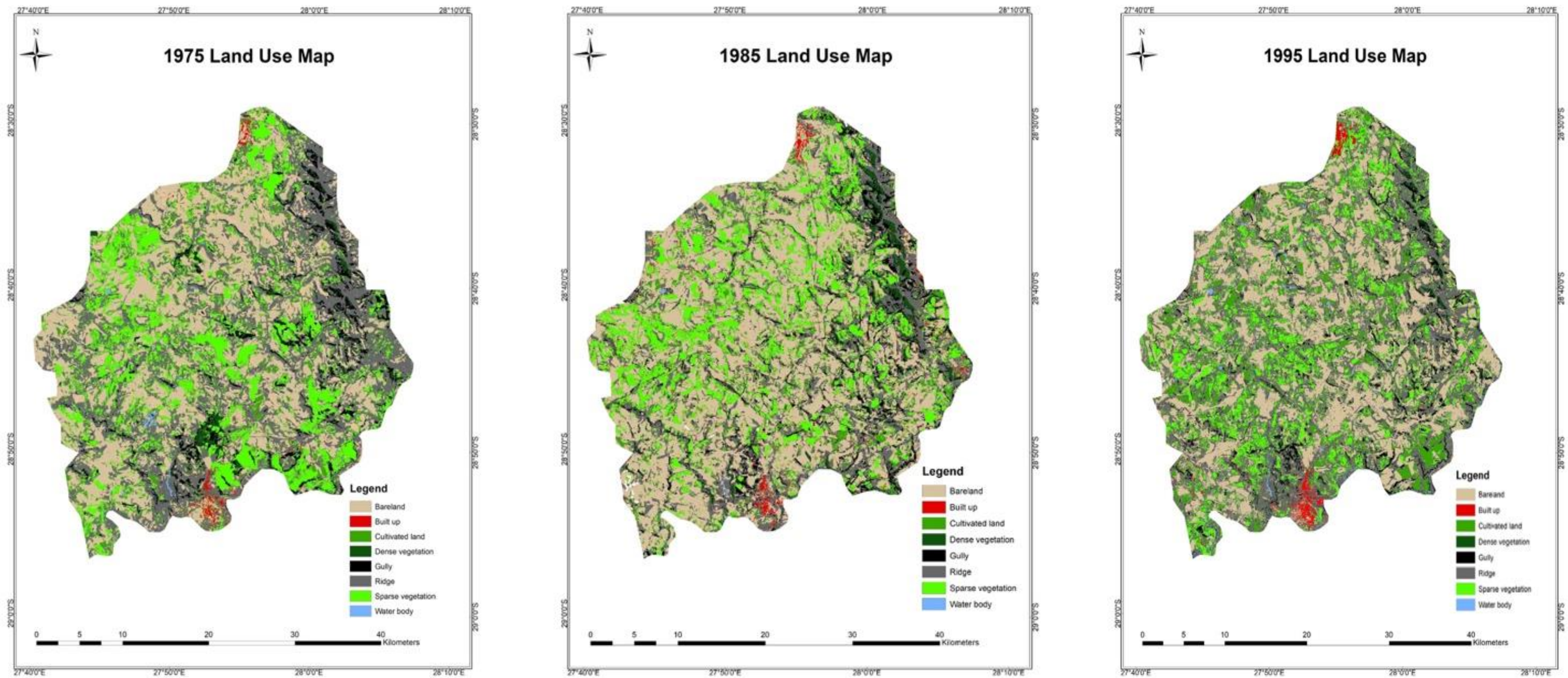

Figure 4a: Mapped land use and land cover (LULC) in the region from 1975 to 1995 in intervals of 10 years.

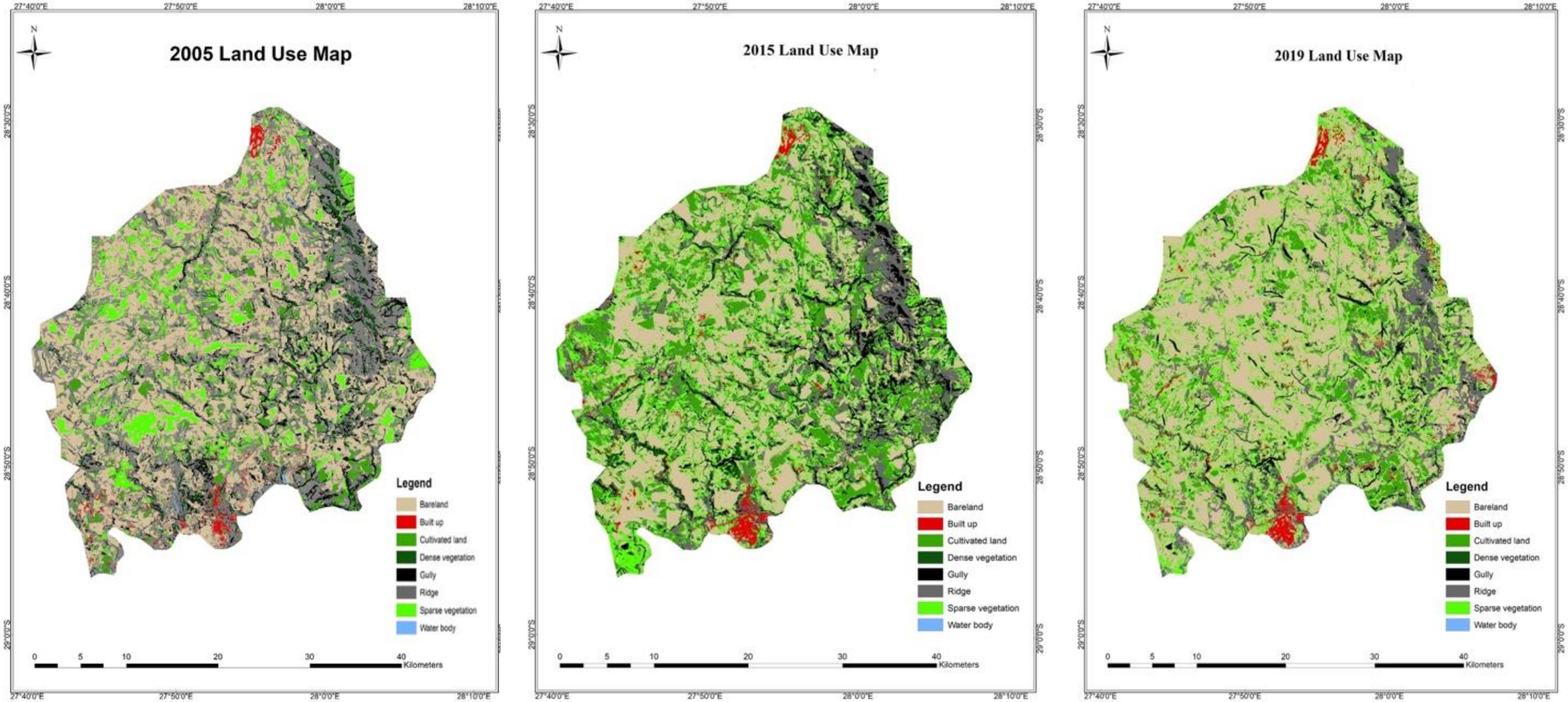

Figure 4b: Mapped land use and land cover (LULC) in the region from 2005 to 2019 in intervals of 10 years.

Figure 5 shows the area covered by gullies and other LULC from 1975 to 2019, as derived from the classification of the Landsat and RF algorithm. In 1975, the dominant land use in Rosendal was sparse vegetation (45.91%), ridge (22.47%) and Bareland (14.43%) while dense vegetation was at least 6.14%, gullied area at 5.32%, cultivated land at 2.99% and built-up and water bodies both below 1.89% each.

In 1985, the dominating land use is sparse vegetation (29.25%), bareland (23.51%) and ridges (22.16%) whilst gullied area is at 10.80%, cultivated land at 6.13% and built-up, dense vegetation and water bodies are covering an area of less than 4% each. In 1995, the dominating land use is sparse vegetation (29.25%), bareland (23.51%) and ridges (23.51%). Gullied area covered at least 10.80 %, cultivated land covered at least 6.13% whilst built up, water bodies and dense vegetation covered less than 4% each.

In 2005, bareland is the most dominating land use covering at least 26.80%, ridge at 22.40%, sparse vegetation at 21.69%, gullied area at 13.28% and cultivated land at 7.09%. Built Up, dense vegetation and water bodies cover less then 5.5% each. In 2015, dominating land use observed is bareland 31.92%, ridges 22.35%, gullied area 15.77% and sparse vegetation 13.51%. Built up covered 8,77%, cultivated land covered 5.64% whilst dense vegetation and water bodies each covered less than 2%. In 2019, dominating land use is bareland at 34.58%, ridges at 22.49%, gullied area at 17.32%, built up at 11.57% and sparse vegetation at 6.68%. Cultivated land covered 5.43% whilst water bodies and dense vegetation cach covered less than 2%.

Figure 5: Land use and land cover change in the region from 1975 to 2019 shown in a histogram. Key: BL= bareland, BU= built up, CL= cultivated land, DV= dense vegetation, GL= gullied area, RG= ridges, SV= Sparse vegetation, WB= water body

Tables 3 to 12 also show the change detection matrices of gullies and associated LULC in the study area from 1975 to 2019. Since 1985, gullied area increased by 2.38%, dense vegetation by 0.01%, while image difference of all other land use classes show decrease ranging from 2.04% to 11.69%. Cultivated land experienced the highest transformation of 42.06% to bareland and 2.23% to gullied area, while sparse vegetation transformed 2.25% to gullied area and 12.81% to bareland. In 1985, many classes experienced high transformation with bareland maintaining 44.95% of its area extent.

In 1995, cultivated land and gullied area increased by 162 ha (2.91%) and 483 ha (5.35%), respectively. Cultivated land experienced the highest transformation of 57.29% transformed to bareland and 4.06% transformed to gullied area. Dense vegetation maintained most of its area (62.84%), while 26.98% of its area transformed to gullied area. Sparse vegetation transformed 17.75% of its area to bareland area.

In 2005, cultivated land had the highest transformation of 33.31% to bareland area and 6.65% to gullied area. Sparse vegetation has the second highest-class transformation with 24.04% transformed to bareland area. Built-up area has a negative image difference showing a decrease of 679 ha (28.45%) while bareland, gullied area and sparse vegetation have a positive image difference showing an increase of 180 ha (0.95%), 87 ha (1.65%) and 150 (0.72%), respectively.

In 2015, sparse vegetation maintained 70.33% (highest) of its area and lost 16.82% to bareland, whereas cultivated land transformed 3.25% of its area to gullied area and 27.85% to sparse vegetation. Built-up area has a negative image difference of 1220 ha (50.68% decrease) while gullied area, bareland and sparse vegetation have a positive image difference showing an increase of 260 ha (3.58%), 2206 ha (9.83%) and 2007 ha (4.14.%), respectively.

In 2019, sparse vegetation maintained 72.57% (highest) of its original area (increase of 2.24% from 2015). Highest transformation of 16.87% of this class was transformed to bareland and 0.47% to gullied area. Cultivated land transformed 41.21% to bareland, 1.38% to gullied area and only maintained 30.36% of its original area (increase of 4.31% from 2015). Built up area has a negative image difference showing a decrease of 1871 ha (30.04%). Bareland, gullied area and sparse vegetation have a positive image difference showing an increase of 2085 ha (10.48%), 491 ha (4.75%) and 1578 ha (3.03%), respectively.

Table 3: Change detection matrix of Gullies (highlighted in gray) and associated LULC types in 1975 to 1985 in hectares, ha.

Land Class		Land Use 1985								Row total
		BL	**BU**	**CL**	**DV**	**GL**	**RG**	**SV**	**WB**	
Land Use 1975	BL	**21062**	4537	2808	9	689	3546	2295	1	34947
	BU	3903	**2100**	380	14	126	1204	773	18	8517
	CL	1384	318	**207**	14	335	488	257	2	3004
	DV	144	22	35	**1043**	136	419	168	28	1995
	GL	353	84	149	1570	**2594**	1956	403	25	7133
	RG	14588	5497	2231	378	4101	**21686**	9678	39	58198
	SV	5341	2595	850	48	682	5509	**4317**	7	19349
	WB	83	96	17	196	142	322	27	**221**	1104
	Grand total	46857	15249	6677	3272	8804	35130	17918	341	
	Gain	25795	13148	6470	2229	6210	13444	13601	120	
	Image difference	-2519	-1783	-173	0	209	-715	-516	-16	

Key: BL= bareland, BU= built up, CL= cultivated land, DV= dense vegetation, GL= gullied area, RG= ridges, SV= Sparse vegetation, WB= water body

Table 4: Change detection matrix of Gullies (highlighted in gray) and associated LULC types in 1975 to 1985 in percentage (%).

Land Class		Land Use 1985							
		BL	**BU**	**CL**	**DV**	**GL**	**RG**	**SV**	**WB**
Land Use 1975	BL	**44.95**	29.75	42.06	0.27	7.83	10.09	12.81	0.26
	BU	8.33	**13.77**	5.69	0.42	1.43	3.43	4.32	5.30
	CL	2.95	2.08	**3.10**	0.43	3.80	1.39	1.43	0.50
	DV	0.31	0.15	0.52	**31.89**	1.54	1.19	0.94	8.30
	GL	0.75	0.55	2.23	47.98	**29.47**	5.57	2.25	7.21
	RG	31.13	36.05	33.41	11.56	46.58	**61.73**	54.01	11.51
	SV	11.40	17.02	12.73	1.46	7.74	15.68	**24.09**	2.07
	WB	0.18	0.63	0.26	6.00	1.62	0.92	0.15	**64.84**
	Grand total	100.00	100.00	100.00	100.00	100.00	100.00	100.00	100.00
	Gain	55.05	86.23	96.90	68.11	70.53	38.27	75.91	35.16
	Image difference	-5.38	-11.69	-2.59	0.01	2.38	-2.04	-2.88	-4.80

Key: BL= bareland, BU= built up, CL= cultivated land, DV= dense vegetation, GL= gullied area, RG= ridges, SV= Sparse vegetation, WB= water body

Table 5: Change detection matrix of Gullies (highlighted in gray) and associated LULC types in 1985 to 1995 in hectares, ha.

Land Class		Land Use 1995								Row total
		BL	**BU**	**CL**	**DV**	**GL**	**RG**	**SV**	**WB**	
Land Use 1985	BL	**17465**	1505	3193	6	658	22470	1546	15	46857
	BU	5395	**2064**	568	5	84	6642	444	46	15249
	CL	1327	96	**731**	3	568	3616	334	3	6677
	DV	1	3	6	**2127**	361	221	29	525	3272
	GL	230	17	226	913	**3981**	3054	352	31	8804
	RG	2524	473	468	295	2725	**25812**	2735	101	35132
	SV	2680	130	375	7	645	10812	**3265**	4	17918
	WB	3	27	7	29	16	55	3	**200**	341
	Grand total	29626	4315	5573	3385	9038	72681	8708	925	
	Gain	12161	2251	4842	1258	5057	46869	5443	726	
	Image difference	-4068	-1968	162	-2	483	-3025	-111	-43	

Key: BL= bareland, BU= built up, CL= cultivated land, DV= dense vegetation, GL= gullied area, RG= ridges, SV= Sparse vegetation, WB= water body

Table 6: Change detection matrix of Gullies (highlighted in gray) and associated LULC types in 1985 to 1995 in percentage (%).

Land Class		Land Use 1995							
		BL	**BU**	**CL**	**DV**	**GL**	**RG**	**SV**	**WB**
Land Use 1985	BL	**58.95**	34.87	57.29	0.17	7.28	30.92	17.75	1.67
	BU	18.21	**47.84**	10.20	0.15	0.93	9.14	5.10	5.00
	CL	4.48	2.23	**13.11**	0.09	6.28	4.98	3.83	0.30
	DV	0.00	0.06	0.10	**62.84**	4.00	0.30	0.33	56.74
	GL	0.78	0.39	4.06	26.98	**44.05**	4.20	4.04	3.35
	RG	8.52	10.96	8.39	8.71	30.15	**35.51**	31.41	10.95
	SV	9.05	3.02	6.72	0.21	7.14	14.88	**37.50**	0.43
	WB	0.01	0.63	0.13	0.86	0.18	0.08	0.04	**21.57**
	Grand total	100.00	100.00	100.00	100.00	100.00	100.00	100.00	100.00
	Gain	41.05	52.16	86.89	37.16	55.95	64.49	62.50	78.43
	Image difference	-13.73	-45.61	2.91	-0.05	5.35	-4.16	-1.27	-4.70

Key: BL= bareland, BU= built up, CL= cultivated land, DV= dense vegetation, GL= gullied area, RG= ridges, SV= Sparse vegetation, WB= water body.

Table 7:; Change detection matrix of Gullies (highlighted in gray) and associated LULC types in 1995 to 2005 in hectares, ha

Land Class		Land Use 2005								Row total
		BL	**BU**	**CL**	**DV**	**GL**	**RG**	**SV**	**WB**	
Land Use 1995	BL	**8254**	484	2711	8	168	12982	4987	31	29626
	BU	1203	**732**	148	7	14	1720	423	67	4315
	CL	1383	52	**1072**	10	101	2351	574	30	5573
	DV	2	2	5	**1211**	1207	897	8	54	3385
	GL	226	18	541	191	**2374**	5300	339	48	9037
	RG	7448	1064	3436	140	1044	**47485**	11813	252	72680
	SV	414	30	225	17	92	5318	**2598**	15	8709
	WB	1	7	2	219	317	126	1	**252**	925
	Grand total	18931	2388	8140	1803	5316	76179	20744	749	
	Gain	10677	1656	7068	592	2942	104874	18146	496	
	Image difference	180	-679	924	2	87	631	150	-37	

Key: BL= bareland, BU= built up, CL= cultivated land, DV= dense vegetation, GL= gullied area, RG= ridges, SV= Sparse vegetation, WB= water body

Table 8: Change detection matrix of Gullies (highlighted in gray) and associated LULC types in 1995 to 2005 in percentage (%).

Land Class		Land Use 2005							
		BL	BU	CL	DV	GL	RG	SV	WB
Land Use 1995	BL	**43.60**	20.26	33.31	0.45	3.16	17.04	24.04	4.10
	BU	6.36	**30.64**	1.82	0.42	0.26	2.26	2.04	8.98
	CL	7.30	2.19	**13.17**	0.53	1.91	3.09	2.77	4.04
	DV	0.01	0.09	0.07	**67.15**	22.70	1.18	0.04	7.24
	GL	1.19	0.73	6.65	10.61	**44.66**	6.96	1.64	6.37
	RG	39.34	44.55	42.21	7.75	19.64	**62.33**	56.95	33.60
	SV	2.19	1.25	2.76	0.95	1.72	6.98	**12.53**	1.96
	WB	0.01	0.28	0.03	12.14	5.95	0.17	0.01	**33.71**
	Grand total	100.00	100.00	100.00	100.00	100.00	100.00	100.00	100.00
	Gain	56.40	69.36	86.83	32.85	55.34	137.67	87.47	66.29
	Image difference	0.95	-28.45	11.35	0.11	1.65	0.83	0.72	-4.94

Key: BL= bareland, BU= built up, CL= cultivated land, DV= dense vegetation, GL= gullied area, RG= ridges, SV= Sparse vegetation, WB= water body.

Table 9: Change detection matrix of Gullies (highlighted in gray) and associated LULC types in 2005 to 2015 in hectares, ha.

Land Class		Land Use 2015								Row total
		BL	**BU**	**CL**	**DV**	**GL**	**RG**	**SV**	**WB**	
Land Use 2005	BL	**8661**	1399	3260	1	116	1722	3771	1	18931
	BU	483	**1286**	75	0	4	277	260	3	2388
	CL	2689	66	**2120**	2	264	731	2267	1	8140
	DV	25	6	15	**645**	155	860	53	45	1803
	GL	209	10	200	677	**2588**	1135	464	33	5316
	RG	15490	836	4401	112	1172	**14700**	39437	31	76179
	SV	3489	122	981	11	77	1473	**14590**	1	20744
	WB	75	47	31	24	15	177	65	**314**	749
	Grand total	31121	3771	11085	1473	4391	21074	60905	429	
	Gain	22460	2485	8964	829	1803	6374	46316	115	
	Image difference	2206	-1220	2045	2	260	454	2007	-2	

Key: BL= bareland, BU= built up, CL= cultivated land, DV= dense vegetation, GL= gullied area, RG= ridges, SV= Sparse vegetation, WB= water body

Table 10: Change detection matrix of Gullies (highlighted in gray) and associated LULC types in 2005 to 2015 in percentage (%).

Land Class		Land Use 2015							
		BL	**BU**	**CL**	**DV**	**GL**	**RG**	**SV**	**WB**
Land Use 2005	BL	**45.75**	20.23	33.03	1.38	3.92	20.33	16.82	10.00
	BU	7.39	**53.84**	0.81	0.34	0.19	1.10	0.59	6.32
	CL	17.22	3.15	**26.05**	0.81	3.77	5.78	4.73	4.19
	DV	0.01	0.02	0.03	**35.75**	12.74	0.15	0.05	3.27
	GL	0.61	0.16	3.25	8.57	**48.68**	1.54	0.37	2.05
	RG	9.10	11.60	8.97	47.69	21.35	**19.30**	7.10	23.60
	SV	19.92	10.88	27.85	2.94	8.72	51.77	**70.33**	8.62
	WB	0.01	0.12	0.01	2.51	0.62	0.04	0.00	**41.95**
	Grand total	100.00	100.00	100.00	100.00	100.00	100.00	100.00	100.00
	Gain	54.25	46.16	73.95	64.25	51.32	80.70	29.67	58.06
	Image difference	9.83	-50.68	25.24	0.47	3.58	4.68	4.14	-2.13

Key: BL= bareland, BU= built up, CL= cultivated land, DV= dense vegetation, GL= gullied area, RG= ridges, SV= Sparse vegetation, WB= water body

Table 11: Change detection matrix of Gullies (highlighted in gray) and associated LULC types in 2015 to 2019 in hectares, ha.

Land Class		Land Use 2019								Row total
		BL	**BU**	**CL**	**DV**	**GL**	**RG**	**SV**	**WB**	
Land Use 2015	BL	**9388**	693	5328	477	807	5650	8768	10	31121
	BU	1005	**1938**	42	24	29	400	313	21	3771
	CL	3090	66	**3926**	130	519	1460	1890	3	11085
	DV	4	1	8	**159**	1198	57	18	30	1473
	GL	115	2	178	460	**3207**	180	246	3	4391
	RG	2048	400	1480	2799	2563	**8688**	3021	77	21075
	SV	4242	248	1962	3960	1867	10893	**37724**	11	60907
	WB	2	18	6	5	136	41	7	**213**	429
	Grand total	19894	3365	12929	8015	10327	27369	51986	367	
	Gain	10507	1428	9003	7856	7120	18681	14262	154	
	Image difference	2085	-1871	3884	106	491	1060	1578	-18	

Key: BL= bareland, BU= built up, CL= cultivated land, DV= dense vegetation, GL= gullied area, RG= ridges, SV= Sparse vegetation, WB= water body

Table 12: Change detection matrix of Gullies (highlighted in gray) and associated LULC types in 2015 to 2019 in percentage (%).

Land Class		Land Use 2019							
		BL	**BU**	**CL**	**DV**	**GL**	**RG**	**SV**	**WB**
Land Use 2015	BL	**47.19**	20.61	41.21	5.95	7.82	20.64	16.87	2.81
	BU	5.05	**57.58**	0.33	0.30	0.28	1.46	0.60	5.68
	CL	15.53	1.97	**30.36**	1.63	5.03	5.34	3.64	0.76
	DV	0.02	0.03	0.06	**1.98**	11.60	0.21	0.03	8.18
	GL	0.58	0.04	1.38	5.74	**31.06**	0.66	0.47	0.70
	RG	10.29	11.87	11.44	34.93	24.82	**31.74**	5.81	20.85
	SV	21.32	7.37	15.17	49.41	18.08	39.80	**72.57**	2.94
	WB	0.01	0.54	0.05	0.06	1.32	0.15	0.01	**58.08**
	Grand total	100.00	100.00	100.00	100.00	100.00	100.00	100.00	100.00
	Gain	52.81	42.42	69.64	98.02	68.94	68.26	27.43	41.92
	Image difference	10.48	-55.61	30.04	1.33	4.75	3.87	3.03	-4.92

Key: BL= bareland, BU= built up, CL= cultivated land, DV= dense vegetation, GL= gullied area, RG= ridges, SV= Sparse vegetation, WB= water body

4.2 Gully erosion analysis and quantification of gully development dynamics from 1975 to 2019

4.2.1 Quantification of gully development in Rosendal since 1975.

Following the use of RF classification algorithm to generate the land use maps of the area, Figure 6 and Table 13 show the long-term changes in gullies and other associated LULC in the study area from 1975 to 2019. Overall, gullied and bareland areas increased by 12% and 21%, respectively. Sparse and dense vegetation show an overall decrease of 39% and 5%, respectively, while cultivated land increased from 1975 to 2005 (from 3% to 7%) and thereafter decreased (from 7% to 5%) especially over the last two decades of the study period. The changes per decade for ridges and water bodies are negligible. In 1975, gullied area covered 5% (79485 ha) of the total study area which increased per decade to 7% (99261 ha) in 1985, 11% (161230 ha) in 1995, 13% (198302 ha) in 2005, 16% (235528 ha) in 2015 and 17% (25870 ha) in 2019 (Figure 6; Table 13). In comparison to other years, the period 1985 to 1995 had the highest change in gullied area (4% increase) compared to the 2% increase 1975 to 1985 and 1995 to 2005 and 1% increase 2015 to 2019.

As the region continued to experience increased gully erosion, bareland also increased from 14% (215458 ha) in 1975 to 35% (516470 ha) in 2019 (Table 13). In 1985, bareland covered 18% and increased by 6% to 24% in 1995 while dense vegetation decreased by 1%. Bareland area further increased to 27% in 2005 and 32% in 2015, making the overall change of bareland area from 1975 to 2019 one of the greatest changes shown in Figure 6 and Table 13. Cultivated land covered 3% of the total area in 1975 and increased to 4% in 1985, 6% in 1995 and 7% in 2005. In 2015, cultivated land area decreased by 1% to 6% and a further 1% decrease to 5% in 2019. Overall, with more increased gullied area and bareland, cultivated land decreased over the years.

Throughout the years, sparse and dense vegetation decreased whilst the overall change in ridges and water bodies is negligible. Dense vegetation covered 6% of the area in 1975 and decreased by 1% per decade until 2005, thereafter decreased by 2% to 1% in 2015 and 2019 (Table 13). Sparse vegetation covered 46% of the total area in 1975, decreased to 40% in 1985 which was followed by a major 11% decrease to 29% in 1995, covering 22% in 2005, decrease by 9% to 14% in 2015 and further decreased to 7% in 2019 (Table 13).
Since 1975, built up area has increased by an overall 10% from 2% in 1975 to 12% in 2019 with greatest 4% increase from the 2005 to 2015 period.

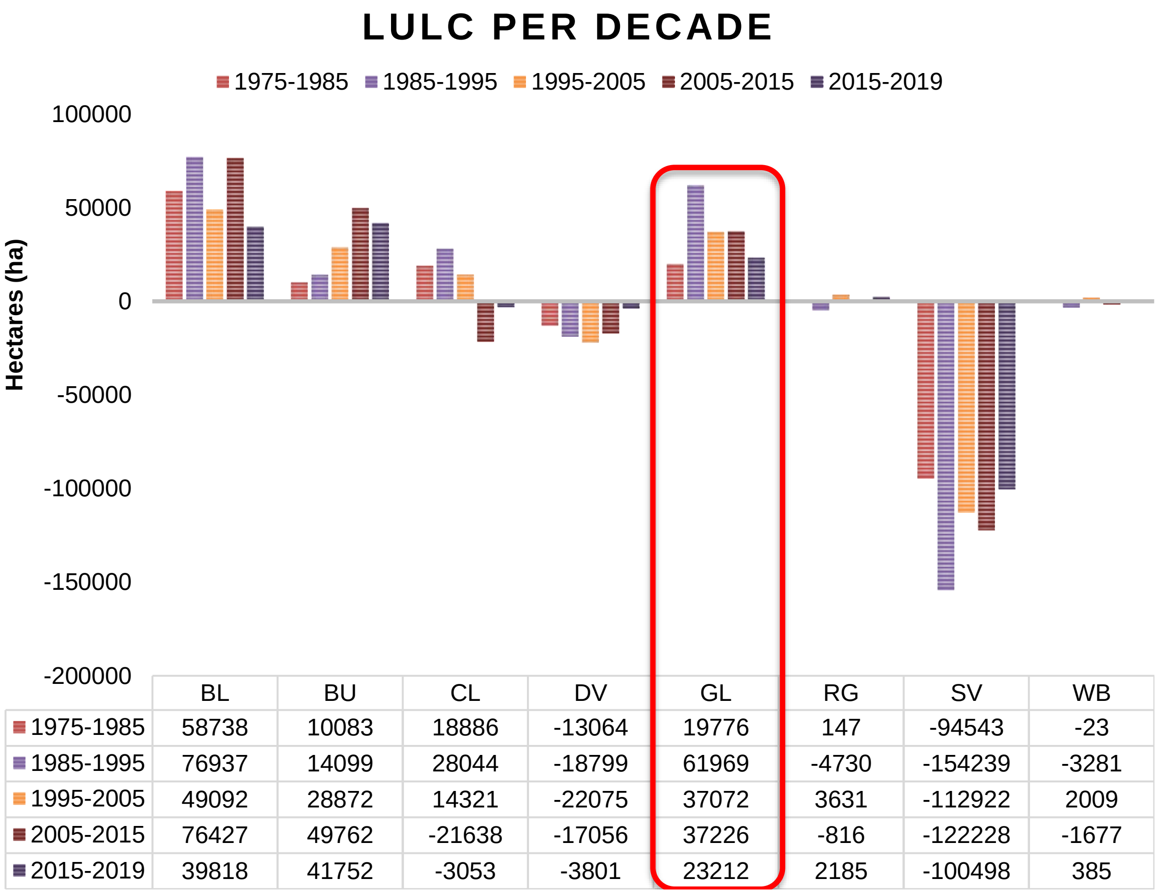

Figure 6: Gullied area (marked in red) and other LULC per decade.

Where BL= bareland, BU= built up, CL= cultivated land, DV= dense vegetation, GL= gullied area, RG= ridges, SV= Sparse vegetation, WB= water body

Table 13: Quantification of the gullied area and other land use changes from the year 1975 to the year 2019.

Land Class	1975		1985		1995		2005		2015		2019	
	ha	%	ha	%	ha	%	ha	%	ha	%	ha	%
BL	215458	14	274196	18	351133	24	400225	27	476652	32	516470	35
BU	28201	2	38284	3	52383	4	81255	5	131017	9	172769	12
CL	44585	3	63471	4	91515	6	105836	7	84198	6	81145	5
DV	91695	6	78631	5	59832	4	37757	3	20701	1	16900	1
GL	79485	5	99261	7	161230	11	198302	13	235528	16	258740	17
RG	335544	22	335691	22	330961	22	334592	22	333776	22	335961	22
SV	685684	46	591141	40	436902	29	323980	22	201752	14	101254	7
WB	12852	1	12829	1	9548	1	11557	1	9880	1	10265	1

Key: BL= bareland, BU= built up, CL= cultivated land, DV= dense vegetation, GL= gullied area, RG= ridges, SV= Sparse vegetation, WB= water body.

4.2.2 Accuracy assessment of the gullied area and other associated land use classes classified maps from 1975 to 2019 in percentages

Table 14 shows the accuracy assessment results of the classification using Random Forest and Landsat images over time. The overall accuracy of the classified maps ranges from 93.95% to 98.17%, with the year 1975 having the highest classification accuracy (98.17%) for the 1975 to 1984 period, and the lowest classification accuracy for the year 1995 (93.95%) for the 10-year period (1995 to 2004). Producer and user accuracy show that the gullied area for the decade starting in 1995 had the lowest producer accuracy of 46.67% and dense vegetation had the lowest user accuracy of 62.5% whilst cultivated land had the highest accuracy (98.98% to 100%) compared to other classes. Gullied area had the highest user accuracy and producer accuracy, together with cultivated land, for the year 1975 and 2019. Kappa Coefficients (KC) range from 92.94% to 97.88% with year 1995 showing lowest KC (92.94%) and year 1975 having the highest KC value of 97.88%.

Table 14: Accuracy Confusion matrices of the gullied area and other associated land use classes classified maps from 1975 to 2019 in percentages (%).

Year	**OA**	**KC**	**AT**	**BL**	**BU**	**CL**	**DV**	**GL**	**RG**	**SV**	**WB**
1975	98.17	97.88	PA	100	98.98	100	100	100	96.81	91.26	99.08
			UA	97.72	98.13	100	95.83	100	97.93	94.84	100
1985	96.41	95.82	PA	100	97.67	100	91.11	80.56	92.80	96.67	100
			UA	99.08	100	100	91.11	85.29	95.08	92.06	100
1995	93.95	92.94	PA	96.58	97.89	100	73.53	46.67	94.32	96.67	100
			UA	99.12	97.89	100	62.5	63.63	94.32	92.55	98.65
2005	96.04	95.37	PA	99.06	99.0	100	66.67	90.63	92.5	94.64	100
			UA	99.05	100	100	85.71	85.29	91.35	94.64	100
2015	97.53	97.13	PA	92.63	98.06	100	93.33	97.87	96.81	98.11	100
			UA	97.77	96.19	98.98	96.55	97.87	95.79	96.3	100
2019	98.12	97.83	PA	95.55	100	100	97.87	100	97.94	95.83	97.99
			UA	97.72	98.16	100	95.83	100	97.93	94.84	100

Key: OA= Overall accuracy, KC= Kappa coefficient, AT= accuracy type, PA= producer accuracy, UA= user accuracy, BL= bareland, BU= built up, CL= cultivated land, DV= dense vegetation, GL= gullied area, RG= ridges, SV= Sparse vegetation, WB= water body.

4.3 Assessing the influence of extreme rainfall conditions on gully development over a long period.

4.3.1 The influence of changes in rainfall patterns, rainfall intensity, and seasonality on gully erosion.

Senekal has a daily rainfall record from 1945 to 2019 with an average total rainfall of 617.84 mm per annum, Ficksburg has a daily rainfall record from 1993 to 2019 with an average total rainfall of 512.07 mm per annum and Bethlehem has a daily rainfall record from 1977 to 2019 with an average total rainfall of 697.58 mm per annum. Average monthly total rainfall received per area from 1945 to 2019 is summarized in Table 15 including indication of the highest and lowest peaks per month in the region.

Senekal received most of its rainfall during the rainfall period of September to April with most rainfall received between December (90.82 mm) and January (101.06 mm) while May to August receive the least amount of rainfall with June and July being the months that received the least amount of rainfall (9.12 mm and 7.59 mm, respectively). Ficksburg received most of its rainfall during the rainfall period of September to April with most rainfall received between December (76.29 mm) and January (88.47 mm) while May to August receive the least amount of rainfall with June and July being the months that received the least amount of rainfall (9.33 mm and 7.12 mm, respectively). Bethlehem received most of its rainfall during the rainfall period of September to April with most rainfall received between December (109.27 mm) and January (120.72 mm) while May to August receive the least amount of rainfall with June and July being the months that received the least amount of rainfall (10.92 mm and 7.87 mm, respectively).

Although the three areas cover different rainfall periods, it is evident that May to August remain the drier period for the region receiving less amount of rainfall, and January (90 mm to 125 mm) and December (75 mm to 110 mm) being months with relatively high total annual rainfall during the rainfall period (September to April) as listed in Table 15.

Table 15: Total average monthly rainfall for the eastern region of Free State from 1945 to 2019.

Month	Bethlehem (1977 to 2019)	Ficksburg (1993 to 2019)	Senekal (1945 to 2019)
	Total average monthly rainfall in mm		
January	120.72	88.47	101.06
February	98.64	67.49	82.66
March	81.00	73.35	79.90
April	45.38	48.14	49.45
May	14.72	18.11	23.18
June	10.92	9.33	9.12
July	7.87	7.12	7.59
August	18.66	12.16	12.39
September	26.08	8.13	20.47
October	72.56	41.70	58.89
November	92.11	61.78	82.31
December	109.27	76.29	90.82

**Red: highest peaks (above 90 mm), *blue: lowest peaks (below 10 mm)*

Figure 7 shows the average total annual and average total monthly rainfall per area. The average total annual rainfall across all areas shows a zig zag pattern (repetitive increase and decline almost every decade) and the average total monthly rainfall shows more rainfall being received September to April compared to the drier months May to August. Some years received lesser rainfall (driest periods) while some received more rainfall (wettest periods) than the normal average rainfall.

In Senekal, since 1945, the year 1945 recorded the lowest average total annual rainfall (11.52 mm) and the year 2006 recorded the highest average total annual rainfall (87.34 mm). In Ficksburg, since 1993, the year 1999 recorded the lowest average total annual rainfall (24.63 mm) and the year 2011 recorded the highest average total annual rainfall (62.25 mm). In Bethlehem, since 1977, the year 2015 recorded the lowest average total annual rainfall (38.78 mm) and the year 2000 recorded the highest average total annual rainfall (81.19 mm).

(

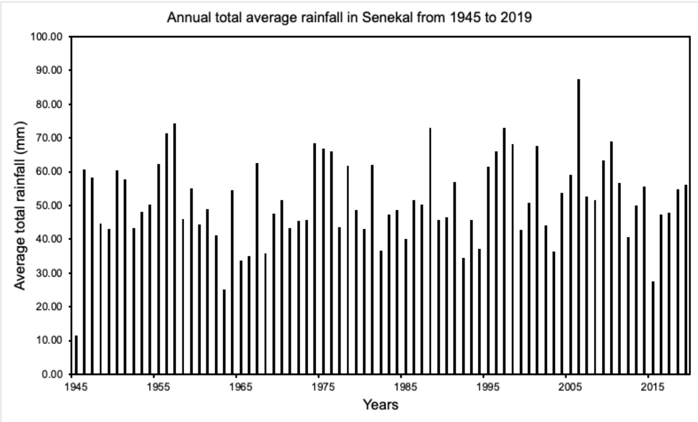

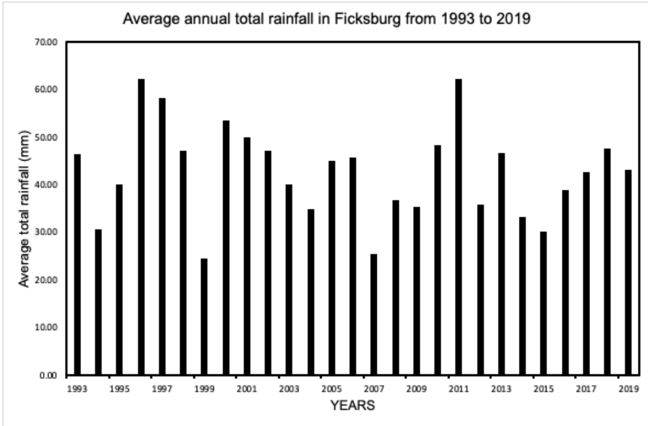

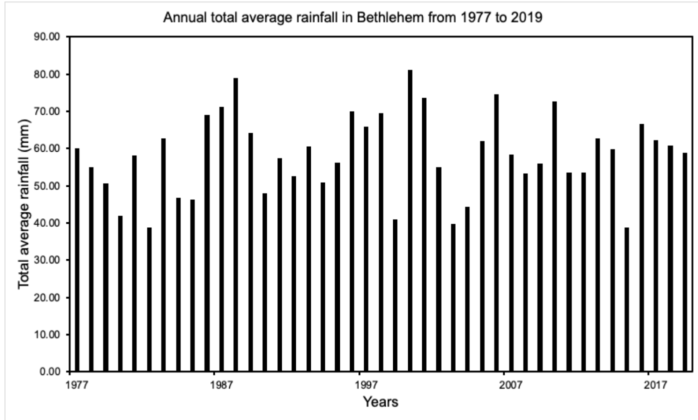

a) Senekal

b) Ficksburg

c) Bethlehem

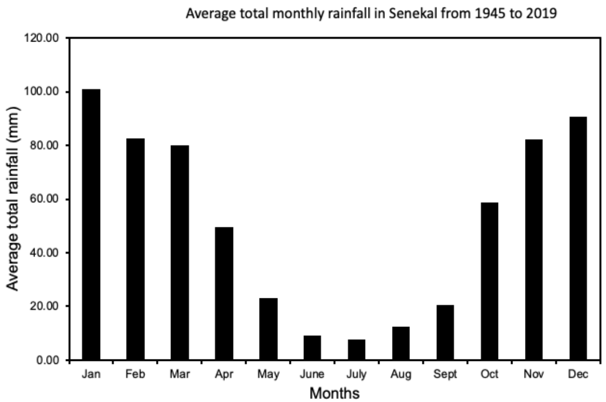

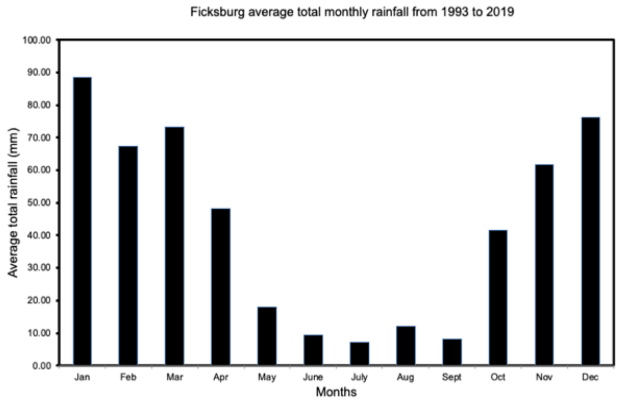

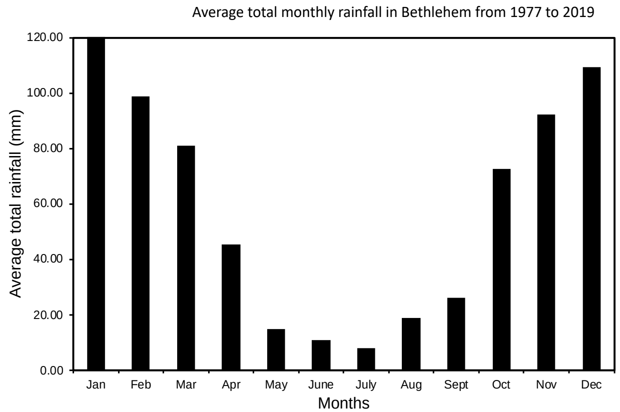

Figure 7: Average total rainfall per area: annual (top) and monthly (bottom). *Where a= Senekal, b=Ficksburg and c=Bethlehem*

Figure 8 also shows the total rainy days (days with more than 1 mm of rainfall received) per year in each area. Senekal is the area with the longest rainfall record, starting in 1945, while Bethlehem's record is from 1977 and Ficksburg has the shortest, starting from 1993. Figure 8 shows the total rainy days per area since 1945 in Senekal, 1977 in Bethlehem and 1993 in Ficksburg.

Since 1945, there are 168 rainy days on average per rainfall period per year which lowers to an average of 167 rainy days per decade. The rainy days per decade are either 4 rain days more or lesser than the previous decade except for extreme changes from 1975 to 1984 (7 rainy days lessor than previous decade) and 1985 to 1994 (10 rain days more than previous decade); which gives an overall of 3 rain days more over the 2 decades from 1975 to 1994.

In Senekal, since 1945, the year 1992 recorded the highest total number of rainy days (180) and lowest total number of rainy days (151) in 2019 (Figure 8: a). In Ficksburg, since 1993, the year 2011 recorded the highest total number of rainy days (180) and lowest total number of rainy days (155) in 2019 (Figure 8: b). In Bethlehem, since 1977, the year 2006 recorded the highest total number of rainy days (181) and lowest total number of rainy days (150) in 1987 (Figure 8: c).

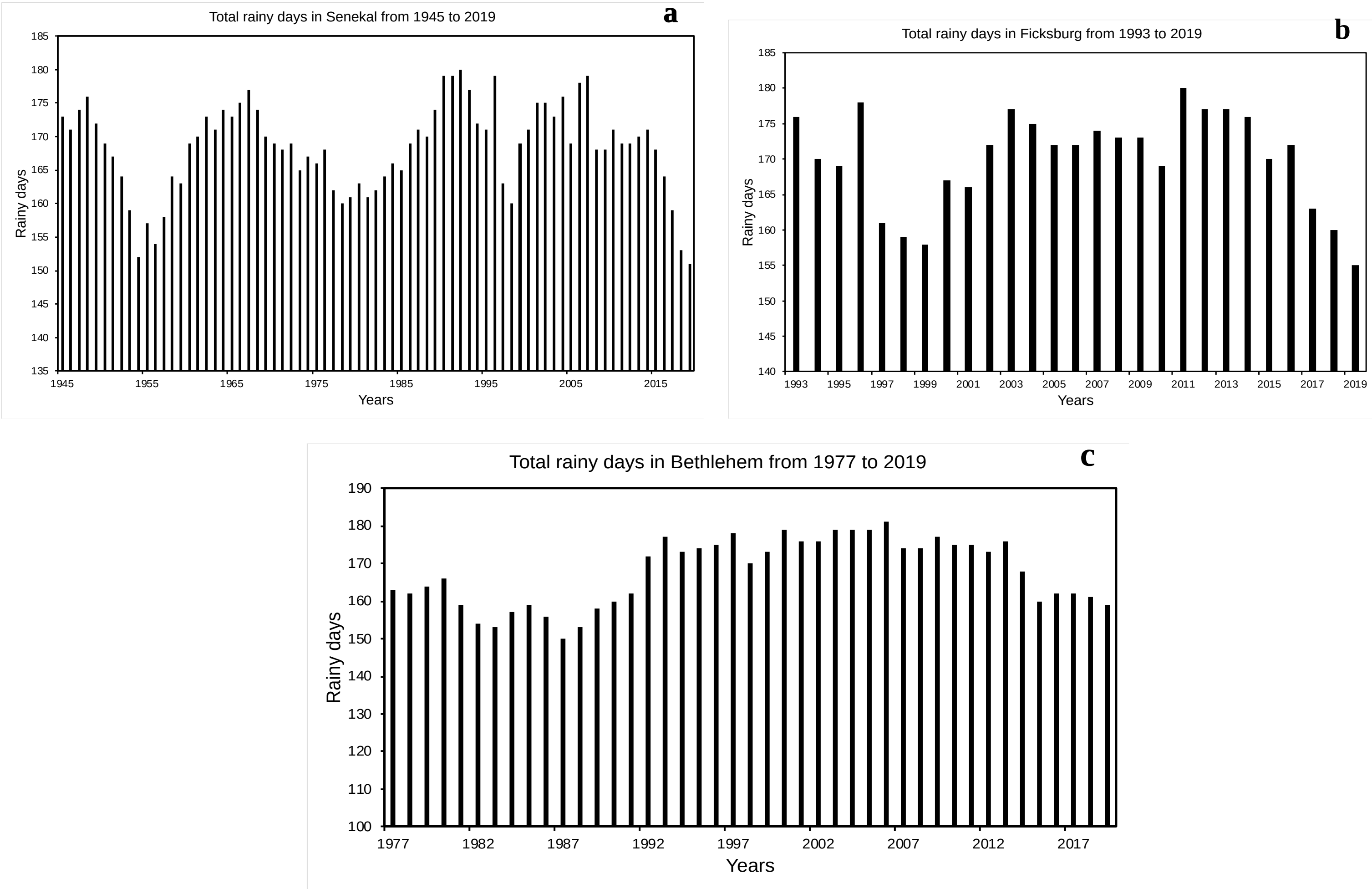

Figure 8: Total rainy days per area.

The rainfall record of these 3 areas overlap between the period of 1993 to 2019 and therefore changes in total rainy days across the region from 1993 to 2019 are shown in Figure 9. Figure 9 (a and b) shows the change in rainy days and average monthly rainfall since 1933 across all areas. From Figure 9a, it is evident that the year 1998 and 2019 recorded the lowest total number of rainy days in all areas. The year 1998 recorded 160 total number of rainy in Senekal, 159 in Ficksburg and 170 in Bethlehem, while in 2019, total number of rainy days were 151 in Senekal, 155 in Ficksburg and 159 in Bethlehem.

Since 1993, most rainfall is still received from September to April and the drier period is May to August annually across all areas as shown in Figure 9b. Despite the noticeable changes from 1995 to 2004 as shown on Figure 9, overall, there was no decadal change in total number of rainy days from the previous decade (1985 to 1994). Since 2005, there has been a continued decrease in the total number of rainy days until 2019.

All areas experience a decreasing trend in the total number of rainy days since 2012 (Figure 9a). The years 1997 to 1999 recorded the lowest total number of rainy days across all areas while the years 2005 to 2006 recorded the highest total number of rainy days in the region (Figure 9). In addition, all areas show a: 1) very low total number of rainy days during the period of 1997 to 2000, 2) decreasing number of rainy days from 2013 to 2019, and 3) another major decrease from 2008 to 2010 in Senekal while the other two areas experienced 4) a steady or slight increase in number of rainy days since 1993 (Figure 9).

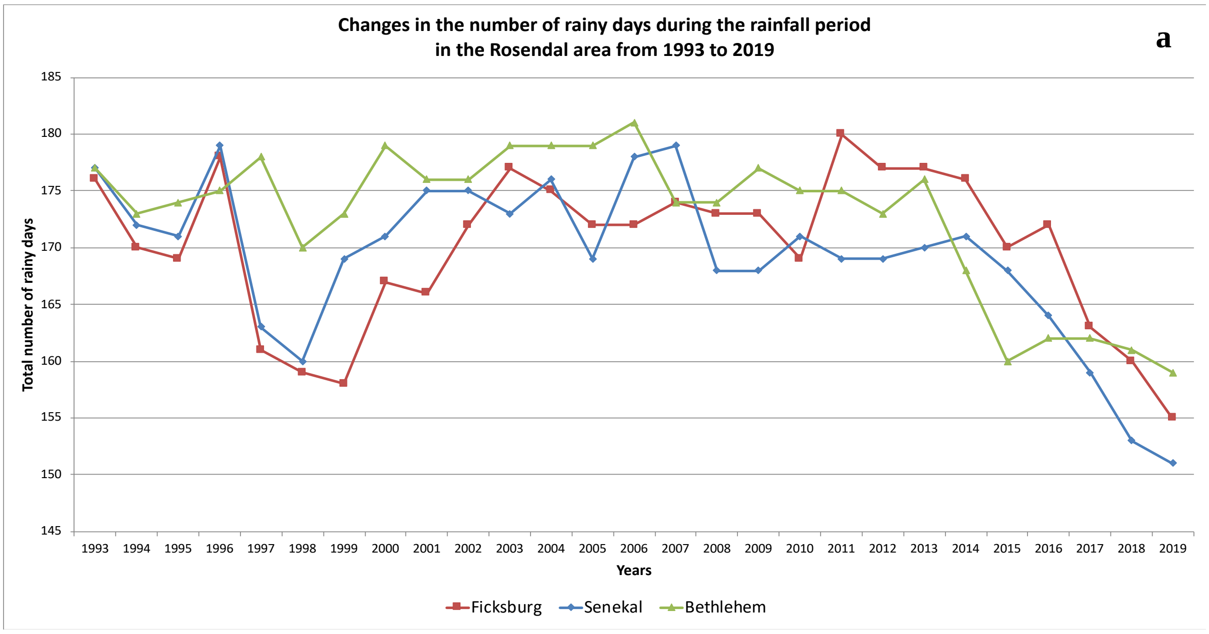

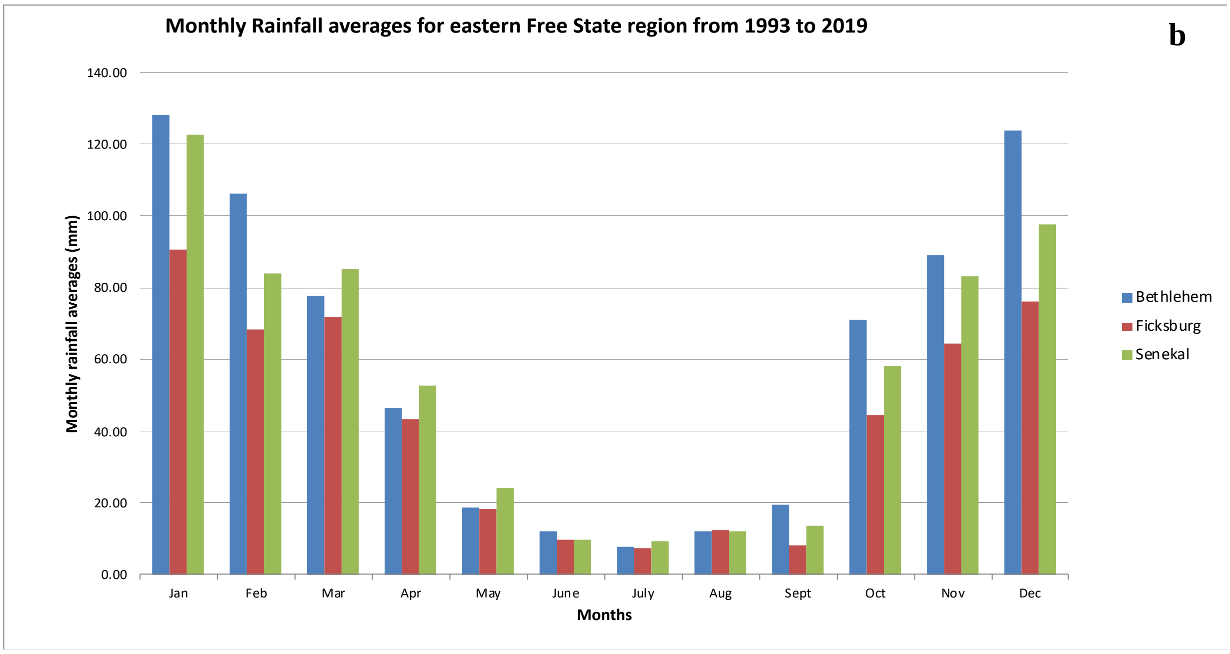

Figure 9: Changes in the total number of rainy days (a), and total average monthly rainfall (b)

Table 16 summarizes the total average monthly rainfall per area since 1993 with highest peaks in red (above 90 mm during rainfall season) and lowest peaks in blue (below 10 mm during dry rainfall season). Table 17 further outlines the long term trends in total rainfall and total number of raindays in the region since 1945. Since 1993, all areas in the region received most of its rainfall during the rainfall period of September to April while May to August receive the least amount of rainfall with June and July being the months that receive the least amount of rainfall. In Senekal, highest rainfall peaks were received in December (123.64 mm), January

(128.05 mm) and February (106.25) and the lowest rainfall peak was July (7.86 mm). In Ficksburg, highest rainfall peak was January (90.45 mm) and lowest rainfall peak were June (9.69 mm), July (7.39 mm) and September (8.16 mm). In Bethlehem, highest rainfall peaks were in January (122.51 mm) and December (97.58 mm) and lowest rainfall peaks were in June (9.79 mm) July (9.20 mm).

Table 16: Total average monthly rainfall for the eastern region of Free State from 1993 to 2019

Month	**Bethlehem**	**Ficksburg**	**Senekal**
	Total average monthly rainfall in mm		
January	128.05	90.45	122.51
February	106.25	68.25	83.90
March	77.56	71.65	85.00
April	46.60	43.32	52.66
May	18.76	18.37	24.21
June	12.05	9.69	9.79
July	7.86	7.39	9.20
August	12.18	12.62	11.97
September	19.42	8.16	13.49
October	70.88	44.29	58.17
November	88.98	64.52	83.33
December	123.64	76.29	97.58

*Red: highest peaks (above 90 mm), *blue: lowest peaks (below 10 mm) and *purple: change (decrease) in highest peak over the past 26 years.

Table 17: Trends in total rainfall and number of raindays for the three areas

Area (rainfall/period)	**Total rainfall (mm)**	**Rainy days**
Senekal (mm/74 years)	**8.35**	**2.27**
Ficksburg (mm/26 years)	- 19.70	- 6.54
Bethlehem (mm/42 years)	**16.61**	**3.99**

Trends in bold are significant at 95% level

Figure 10 shows the rainfall intensity in the region based on the average rainfall intensity of the highest four events and rainfall events recorded in the highest 5% throughout each rainfall record per area. Highest rainfall intensities were recorded in 1974 (Senekal), 2011 (Ficksburg) and 2010 (Bethlehem. Lowest rainfall intensities were recorded in 1945 (Senekal), 1999 (Ficksburg) and 1982 (Bethlehem).

The two approaches used to calculate extreme intensity show positive linear trends with the index calculated through the average of the highest 5% events showing a stronger positive trend. The average of the highest 4 events per year (solid line) and average of the highest 5% of events (dashed line) show an agreement the region with positive increasing trends in each area.

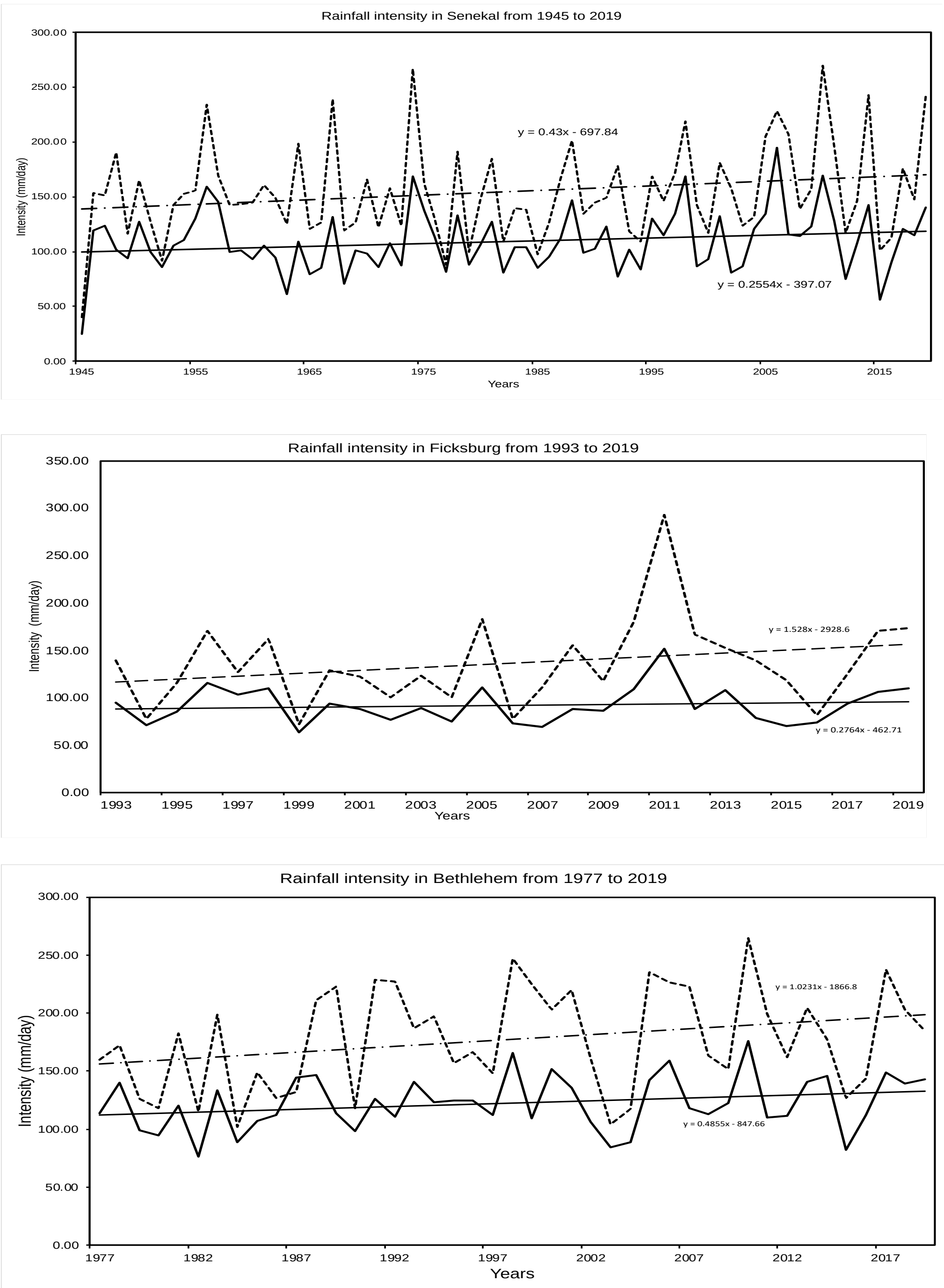

Figure 10: Average intensity of the 4 highest events (solid line) and highest 5% (dashed line) of events in the region with linear trends.

4.3.2 Extreme rainfall events, rainfall anomalies and their impact on gully development in the area

The eastern region of Free State Province has a mean annual rainfall of 577.78 mm in Bethlehem, 410.38 mm in Ficksburg and 436.76 mm in Senekal. Since 1945, the area has either received higher or lower than the normal annual average rainfall during the rainfall period. Table 18 summarizes the rainfall anomalies per area in the region to show the years (or periods) where either more or lesser rainfall was received.

The driest periods in Table 18 are the rainfall periods in all areas from 1945 to 2019 (Senekal), 1977 to 2019 (Bethlehem) and from 1993 to 2019 (Ficksburg) where the three different areas received average monthly rainfall very much lower than the usual and thus marked as the driest periods. The years 1981 to 1985 and 2015 to 2016 were the driest years in the region. The years 1993 to 1997 and 2010 to 2011 were the wettest years. These are rainfall periods where more rainfall was received than the normal annual average rainfall.

Table 18: Wettest and Driest periods in the eastern region of Free State from 1945 to 2019.

Area	**Average annual rainfall in mm**	**Wettest rainfall period (where 1 is the highest rank)**			**Driest rainfall period (where 1 is the highest rank)**		
		1	**2**	**3**	**1**	**2**	**3**
Bethlehem	577.78	1993-1994	1987-1988	2001-2002	1981-1982	2015-2016	1994-1995
Ficksburg	410.38	1996-1997	2010-2011	2017-2018	2015-2016	2009-2010	1994-1995
Senekal	436.76	1996-1997 & 2010-2011	1956-1957	2007-2008	1982-1984	1962-1963	1981-1982

Time series of changes in extreme rainfall events has been calculated for each area for the period of January 1945 to December 2019 by determining rainfall indices. These changes in extreme events were calculated to identity the months and years where extreme rainfall was received, frequency of the occurrence of these extreme events and the intensity of the extreme events. The occurrence of the extreme events above the 95th percentile and the highest four extreme events occur during the rainy season from September to Aril per year with more extreme events occurring from November to February annually.

In some rare cases, extreme rainfall events occurred during the drier season (May to August) in Senekal (July 2016), in Ficksburg (May 1997 and August 2006) and in Bethlehem (July to August 1980). A summary of the extreme indices in the region for all three areas are listed in Table 19 showing the extreme frequency per month across the three areas in the region during the rainy period. In Senekal, lowest occurrence of extreme rainfall events was in October (4.17%) and highest occurrence was in January (23.61%). In Ficksburg, lowest occurrence of extreme rainfall events was both in October and February (6.25% each) and highest occurrence was in December (25.00%). In Bethlehem, lowest occurrence of extreme rainfall events was in March (11.63%) and highest occurrence was in January (23.26%).

Table 19: Extreme frequency per month in each area over time

Months	**Senekal (1945 to 2019)**	**Ficksburg (1993 to 2019)**	**Bethlehem (1977 to 2019)**
October	4.17%	6.25%	13.95%
November	16.67%	15.63%	16.28%
December	19.44%	25.00%.	16.28%%
January	23.61%	15.63%	23.26%.
February	12.50%	6.25%	18.61%
March	15.28%	15.63%	11.63%

Table 20 also shows extreme rainfall events by summarizing trends in rainfall indices: extreme intensity, extreme percent, and extreme frequency in the region for each area. The number of extreme events (frequency) strongly increased in Senekal and Bethlehem since 1975 and 1977, respectively, while strongly decreasing in Ficksburg since 1993. Extreme intensity of rainfall events strongly increased in Senekal and Bethlehem while negligibly decreased in Ficksburg. The proportion of the total rainfall from extreme events (extreme percent) strongly increased in Ficksburg while negligibly decreased in Senekal and Bethlehem.

Table 20: Trends in extreme intensity, extreme percent and extreme frequency calculated using three different methods for the three areas. *Bold values represent significance at 95%.*

Region (period)	**Annual top four events**		**Annual top 5%**		**>Long-term 95th percentile**		
	Extreme intensity (mm)	Extreme percent (%)	Extreme intensity (mm)	Extreme percent (%)	Extreme intensity (mm)	Extreme percent (%)	Extreme frequency (days)
Senekal (per 74 years)	**1.48**	0.18	**2.09**	0.25	1.81	- 0.24	**0.97**

Region (period)	**Annual top four events**		**Annual top 5%**		**>Long-term 95th percentile**		
	Extreme intensity (mm)	Extreme percent (%)	Extreme intensity (mm)	Extreme percent (%)	Extreme intensity (mm)	Extreme percent (%)	Extreme frequency (days)
Ficksburg (per 26 years)	- 3.53	0.18	- 5.25	**0.27**	- 4.34	**0.23**	**- 1.23**
Bethlehem (per 42 years)	**2.91**	0.18	**4.22**	0.26	3.66	- 0.23	**1.02**

Since 1945 to 2019, extreme events and rainfall anomalies have been occurring in Rosendal, with more extreme events in some years and shorter rainy days in some years (vice versa). The years 1981 to 1984, 1993 to 1997, 2009 to 2011 and 2016 were the years with the most extreme events. This corresponded to the periods that experienced increased gully erosion (as indicated by increased gullied area), with increased sparse vegetation and bareland area across the region. Figure 11 shows gully development and occurrence of extreme rainfall events in the area from 1975 to 2019; where Senekal rainfall data covered records from1975, Senekal and Bethlehem from 1977, and all three areas from covered records from 1993, and Table 21 summarizes these observed changes in gully development and rainfall events in the area.

Looking at Figure 11 (a and b) and Table 21; from 1975, there has been increased gully erosion resulting to an increase in total area covered by gullies. In 1975, gullied area covered 5% of the total area and about 18% of rainfall events that occurred were recorded extreme. In 1985, gullied area increased by 2% to 7% while recorded occurrence of extreme events remained at 18% over the past decade. With more gully erosion and extreme rainfall events occurring, gullied area further increased to 11% in 1995 (increase of 4% from 7% of the previous decade), with a 3% increase in occurrence of extreme rainfall events from 18% of the previous decade to 21% in 1995. In 2005, gullied area increased to 13% and occurrence of extreme events decreased to 19%. In 2015, gullied area increased to 16% and further increased to 17% in 2019, while occurrence of extreme rainfall events increased to 20% in 2015 and decreased to 14% in 2019.

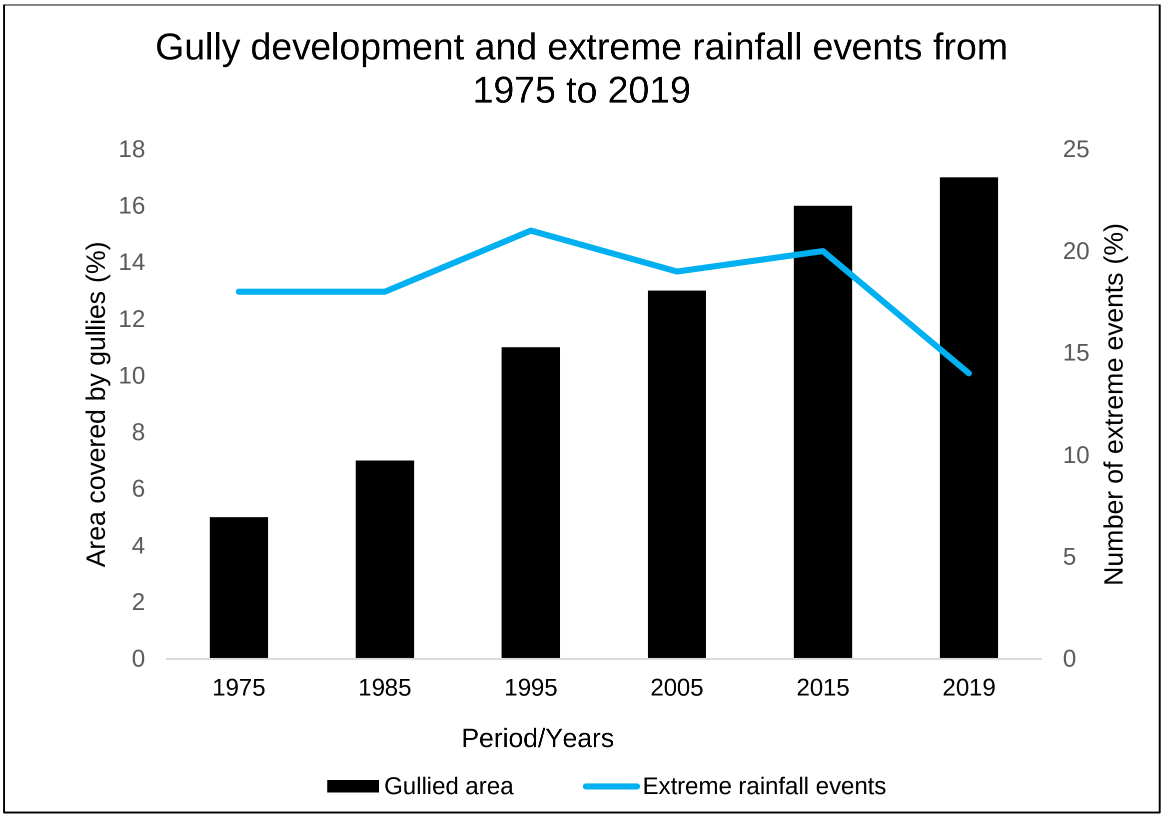

Figure 11a: Gully development and occurrence of extreme rainfall events.

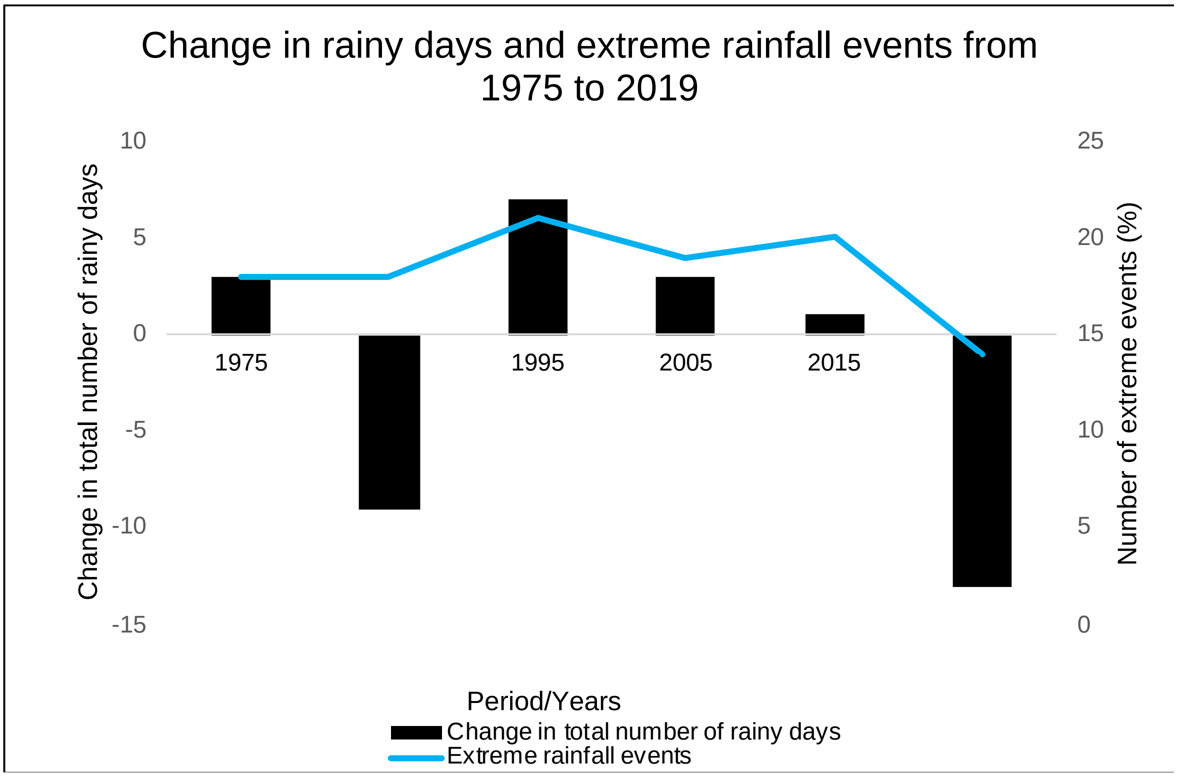

Figure 11b: Change in rainy days and extreme events from 1975 to 2019

Table 21 also shows gully development and extreme rainfall events from 1975 to 2019 including the change (increase or decrease) in number of rainy days during the rainfall period of each decade. In 1975, the rainfall period was longer by 3 days compared to the previous decade, while occurrence of extreme rainfall events reported remained at 18% and gullied area cover increased. By 1985, the rainfall period reduced by 9 days. In 1995, 2005 and 2015, rainfall period increased by 7 days (with increased occurrence of extreme events by 3%), 3 days (decreased occurrence of extreme events by 2%) and 1 day (with increased occurrence of extreme events by 1%), respectively, with increased gully activity per decade listed in Table 21.

Table 21: Gully development and extreme rainfall events from 1975 to 2019.

Years (per decade)	**Area covered by Gullies (%)**	**Number of extreme events (%)**	**Change in number of rainy days (increase or decrease)**
1975	5	18	+3
1985	7	18	**-9**
1995	**11**	**21**	**+7**
2005	13	19	+3
2015	16	**20**	+1
2019	**17**	**14**	**-13**

Note: Where change in number of rainy days- decrease (-) and increase (+). Bold values represent significant changes in gullies and rainfall events.

CHAPTER 5: DISCUSSION

Gully erosion is an important type of soil erosion in areas exposed to overgrazing and characteristic of highly erodible soils as it hinders soil fertility, destabilizes the topsoil, and affects any farming activities in areas dependent on farming (Kuhn, 2013). Different remote sensing mapping techniques have been applied in gully development studies and more intensely in studies focusing on land use and land cover (LULC) changes at a regional scale (Taruvinga, 2008). Over the years, with advancement in RS approaches applied, application of more robust practices for change detection of LULC have provided new understanding of mapping and quantifying gully development and other LULC classes to analyse changes over a long period (Ferrer et al., 2017). This study has investigated, determined, and shown that land use change detection, through remote sensing of gullies and other associated LULC, is a crucial and more practical approach for land management at local scale.

Classification statistical analysis of the six mapped images for 1975, 1985, 1995, 2005, 2015 and 2019 showed a continuous increase in gullied area, bareland area and built-up area with a continuous decrease in sparse vegetation. Cultivated land portrayed an increase from 1975 to 2005 and thereafter a decrease in cover from 2005 to 2019. Over the 44 years, gullied area increased from covering 79 485 ha (5%) to 258 740 ha (17%) of the total area with cultivated land being the main LULC class transforming to gullied area. Areas with sparse vegetation and bareland are the other main contributors detected to transforming to gullied area. The increased gullied area in the region associated with cultivation can be assumed to be as a result of overgrazing (Mararakanye & Le Roux, 2012), which has led to unsustainable land management practices in the region (Meadows & Hoffman, 2003; Kuhn, 2013). Consequently, more land in the area has been exposed to intense gully erosion causing increased gully systems, decreased vegetation cover, and exposing more highly erodible soils to erosion in areas now covered with sparse vegetation or bareland.

This study found reduced cultivated land in the area with increased gully activity in Rosendal. The increase in gullies in the area continues to create more farming challenges for the local community due to decreased available land for cultivation since 1975. As a result of increased gully development in the area, less land is available to the local farmers for cultivation and increased risk for livestock when the gully systems collapse (Taruvinga, 2008; Kuhn, 2013). The findings of this study will help the local community and authorities to better manage their land and use the classified images for further research on possible soil piping in the area. Using the classified mapped images, the local community will be able to see which parts of the area the gully systems are increasing from 1975 to 2019, thus allowing them to incorporate plans for stabilizing and rehabilitation of the area in their local land management practices as well as improving their farming practices (Kuhn, 2013; Ferrer et al., 2017, Perez & Garcia, 2017).

From all the classified maps, the area has been classified into eight (8) classes per decade since 1975 and these were accurately distinguished with overall accuracies ranging from 93.95% to 98.17% and Kappa Coefficients ranging from 92.94% to 97.88%. The use of RF algorithm and Landsat images to classify and map gullies during this study has therefore shown strong capability and credibility of using RS in mapping gullies and change detection over a long period of time. The lowest accuracy assessment values for gullied area (46.67% PA and 63.63% UA) and dense vegetation (62.50% UA) for the year 1995, and dense vegetation (66.67% PA) in 2005 could be a result of mixed pixels that caused misclassifications due to similar spectral reflectance of the images, hence low UA and PA. In addition, the high transformation value of 36.05% from built up area to ridges in 1985 and high sparse vegetation to ridges class transformation (56.96%) in 2005 could also be a result of misclassification. The misclassification and possible low accuracies due to mixed pixels caused by similar spectral reflectance of images is expected due to challenges associated with spatial heterogeneity at local scale which is even a bigger challenge at regional scale (Ferrer at., 2017). Furthermore, although bareland areas include rocky outcrops, the interpretation and analysis of bareland areas with open fields is problematic during the dry period (mid-autumn to early spring: mid-May to early September) (Chase & Meadows, 2007; Rwanga & Ndambuki, 2017; Ferrer et al., 2017), as both classes exhibit similar spectral response (Ferrer et at., 2017).

Furthermore, this project also determined the influence of changes in rainfall patterns and rainfall intensity on gully development at a local scale. The results presented annual and monthly rainfall patterns in Rosendal from 1945 to 2019 with most of the rainfall recorded between September and April annually, and the drier period running from May to August. December and January receive the most rainfall, whilst June and July receive the least rainfall. South Africa receives rainfall seasonally across the country with some parts receiving rainfall in Summer (Summer Rainfall Zone- SRZ), all year-round rainfall (YRZ) and winter rainfall zone (WRZ), and each rainfall zone influences farming activities and land management (Roffe et al., 2020). As outlined by Chase and Meadows (2007) and Roffe et al. (2020), the Free State region falls under the SRZ. The SRZ is characteristic of heavy summer seasonal rainfall (December to February), and very cold and dry winter seasons (June to August) (Chase & Meadows, 2007). Autumn (March to May) and spring (September to November) are also characteristic of rainfall in some parts of South Africa such as the Rosendal area in eastern

Free State region (Chase & Meadows, 2007; Kuhn, 2013). While the region continues to receive rainfall within the wet season, this study has shown the changes and shifts being experienced by the region regarding the duration of the rainfall period and the intensity of the rainfall. Overall, the rainfall period (September to April) received very little (driest period) rainfall in 2015 to 2016, 1981 to 1984 and 1994 to 1995 and the wettest rainfall periods are 1993 to 1994, 1996 to 1997 and 2010 to 2011. Throughout record (from 1945) and most recently over the past 26 years (from 1993), the eastern region of Free State continues to experience extreme events over a shortened rainfall period with total number of rainy days significantly decreasing since 1993. These short- and long-term changes in seasonality in the area can potentially influence the natural geomorphological processes and agricultural activities occurring in an area. This can possibly be due to the global climate change triggering shifts in rainfall patterns with the most vulnerable regions (developing countries) experiencing the most severe impacts (Meadows & Hoffman, 2003; Han et al., 2017).

Since 1993, findings of this project have shown that extreme rainfall events continue to occur in the area over a shorter period leading to the experienced extremely wetter and drier periods. As a result of increases and decreases in rainy days annually; rainy days are either 9 days more or lesser between the decades except major change from 1997 to 2006 where in overall the rainy days were 11 days more than the previous decade. Before 1992, rainy days per year are much lower than from 1992 to 2006, and since 2007 there has been a decrease in the number of rainy days. The *decreased* total number of rainy days from 1996 to 1999 and 2007 to 2011 coupled with the *wettest period* being 1996 to 1997 and 2010 to 2011 shows that during these two periods since 1993, *high* amount of rainfall was received over a short period of time in the Rosendal area. Consequently, this intense amount of extreme rainfall over a shorter period can be assumed to be the main cause for the increased gullied area cover from 7% to 11% in 1995 because the changes in total number of rainy days directly influences the rainfall intensity due it its sensitivity to changes in rain days (Haylock & Nicholls, 2000) and directly influences soil erosion (Han et al., 2017). Overall decrease in total number of rainy days with decreased and/or increased rainfall occurrence and intensity, and increased number of rainy days with decreased and/or increased rainfall occurrence and intensity, has a direct impact on gully development which can lead to increased gullied area and/or bareland area (Han et al., 2017).

The presented rainfall results in this study on extreme rainfall events over the years from 1945 to 2019 have also shown that extreme rainfall events occurred in 1993, 2005 to 2006, 2010 to 2013 and in 2016. Most of the observed extreme rainfall events occurred during the rainfall period (September to April) annually with few exceptions that occurred outside this period in

July 2016 in Senekal. Since 1945, the number of extreme rainfall events (frequency) and extreme intensity has significantly increased in Senekal and in Bethlehem since 1977, while extreme percent (proportion of the total rainfall above extreme rainfall events) has significantly decreased. This suggests that total rainfall received in the area is increasing at a proportionally greater rate (Haylock & Nicholls, 2000), thus, making areas with increased bareland and sparse vegetating more vulnerable to gully erosion. The observed stronger positive trend with the highest 5% approach across all the areas in the region is expected due to the reduction in the number of rainy days since 1993 while increased frequency of extreme events still occurs during the rainy period. This is due to the sensitivity of rainfall intensity to changes in total number of rain days (Haylock & Nicholls, 2000).

The influence of rainfall extreme events on gully development needs to be prioritized in mapping and monitoring gully development in areas exposed to extreme rainfall events (Han et al., 2017), especially in developing areas experiencing unsustainable land management practices (Kuhn 2013). During mapping of these gully systems, application of robust RS and GIS measures is crucial to ensure appropriate understanding of gully morphology in the area (Seutloali et al., 2015, Ferrer et al., 2017). As a result of continued gully development and exposure of bareland, cultivated land has decreased over the decades and some built-up area (domestic and commercial) is gradually growing in some areas especially around town and in some farms. Most of the gullies are expanding near cultivated land, along the ridges and rivers with increased bareland and sparse vegetation proximal and/or within these gullied systems. Findings of this study can help local community management with understanding and integrating the years showing intense increased gully erosion coupled with increased rainfall intensity (in 1974, 2010 and 2011) or reduced rainfall period (1997 to 1999). This will help improve local land management in different aspects such as land use, crop production and grazing (Taruvinga 2008, Kuhn 2013), especially development of policies focused on land use (Meadows & Hoffman, 2003).

CHAPTER 6: CONCLUSION AND RECOMMENDATIONS

6.1 Conclusion

The aim of this study was to determine the spatial and temporal characteristics of gullies from 1975 to 2019 in the Rosendal, eastern Free State, South Africa. This was done through mapping and analysis of gullies and other associated land use and land cover changes using multi temporal Landsat data of 10-year intervals. This study further quantified the dynamics of gully development and assessed the influence of extreme rainfall conditions on gully development. This study has demonstrated that better understanding of gully development can be determined through analysis and integration of remote sensing and climate variables. This was achieved through use of remote sensing land use and cover changes to detect changes in gully development and integrating it with identified changes in climatic conditions, focusing on extreme events, at a local scale, over longer periods of time. The land use and cover change results showed an overall increase in gullied areas (12%) and bareland (21%). On the other hand, decreased cultivated land (slightly increased by 2% from 1975 to 2005 with a 1% decrease since 2015) and vegetated land (5% decrease in dense vegetation and 39% decrease in sparse vegetation). Results further showed increased extreme rainfall intensity and occurrences in the area. In addition, there was an association between extreme events and gully development. The years 1993, 2010 to 2011 and 2016 were the periods with increased gullies and increased extreme wetter rainfall events, while the periods 1981 to 1984 and 2015 to 2016 have the extreme drier rainfall periods with increased gullies and bareland in the area. As a result of the increase in extreme rainfall events and gully development in the area, it can be concluded that the amount of available land for farming in the area has decreased over the decades. This negatively impacts both domestic and commercial agricultural practices in the area.

6.2 Limitations

Although sufficient data was available for this study, limitations on availability of historical Landsat images makes it hard to cover more years to determine longer term changes in the region. In addition, a study covering the dynamics and changes of landscape will have limitations due to the complexity of nature, such as gullies being three dimensional and changes in gully surface area can occur without any net exportation of sediment from the system, thus making it hard to simplify some external factors through modelling or mathematical equations (Rwanga & Ndambuki, 2017). Furthermore, although bareland areas include rocky outcrops, the interpretation and analysis of bareland areas with open fields is problematic during the dry period (mid-autumn to early spring: mid-May to early September) (Chase & Meadows, 2007; Rwanga & Ndambuki, 2017; Ferrer et al., 2017), as both classes exhibit similar spectral response (Ferrer et at., 2017). Rainfall data availability challenges were also encountered, due to limited available rainfall stations in the region, as well as having some parts of the regions with limited available data for the long-term period due to fewer stations pre-1990. Due to data availability limitations, applied calculation methods for comparing different periods could potentially influence the results due to differences in available data.

6.3 Recommendations

Further research is required at a local scale to fully outline the dynamics of gully systems in areas close to cultivated land. Key findings from this study can help future studies focusing on local scale understanding of gully development and identification of vertical soil pipping in gully systems in areas experiencing soil piping. This includes field data collection as part of ground truthing to identify and measure some gully systems. Future studies looking into influence of rainfall and other climate variables on gully development at local scale should make use of remotely sensed rainfall products to avoid data availability challenges from rainfall stations. Future studies looking into future projections of the climate and gully development in the area would be crucial for the local farmers, better land management and most importantly, disaster management practices in the area.

Governance and policies

Socio-economic issues and applied policies play a huge role in land management especially in areas vulnerable to erosion, mass movements and urban development. Ensuring sustainable development and monitored management practices is crucial to eliminate mismanagement of resources and environmentally non-friendly activities in the area. Therefore, incorporation of land use policy and anthropogenic practices is crucial for future studies aimed at projecting and modelling future changes in land use and land cover change. In the ongoing application of the Sendai Framework aimed at disaster risk management at local scale, more geomorphological research on key issues such as gully development at local scale regional is needed to help improve disaster management measures and responses. The landscape naturally experiences geomorphic processes, change and responses. Anthropogenic practices, especially agriculture, accelerate the process in a negative response mechanism where unsustainable measures are applied. To help better manage the agricultural practices in Rosendal and many areas dominated by farming; more desktop, field and practical work is needed to ensure local communities better manage their land in cooperation with local to national governing bodies to avoid delayed response or late reactions to hazardous incidents due to gully development.

References

Abdi, O.A., Glover, E.K. and Luukkamen, O. 2013. Causes and Impacts of Land Degradation and Desertification: Case Study of the Sudan. *International Journal of Agriculture and Forestry.* 3 (2): 40-51.

Akhtar-Schuster, M., Stringer, L.C., Erlewein, A., Metternicht, G., Minelli, S., Safriel, U. and Sommer, S. 2017. Unpacking the concept of land degradation neutrality and addressing its operation through the Rio Conventions. *Journal of Environmental Management.* 195 (1): 4-15

Almeida-Warren, K., Braun, D.R. and Carvalho, S. 2021. The DistoX2: A methodological solution to archaeological mapping in poorly accessible environments. *Journal of Archaeological Science: Reports.* 35: 102688

Alsalman, A.S., Mattar, H.E., Ali, A.E., 2010. Comparative Study of Change Detection and Urban Expansion Using Multi-Date Multi-Source Data: A Case Study of Greater Khartoum 34.

Bader, C. J. (Ed.). 1962. Typical soils of the East London district; the border region, natural environment and land use in the Eastern Cape. Cape Town: *Oxford University Press*. [Available online].

Bagan, H. and Yamagata, Y. 2012. Landsat analysis of urban growth: How Tokyo became the world's largest megacity during the last 40years. *Remote Sens. Environ*. 127: 210–222.

Bands, D. P. 1985. The influence of mountain catchment area control measures on land management in the groot-Winterhoek area of the Western Cape: ecological, economic and social implications. (Doctoral dissertation, University of Stellenbosch).

Bell, F.G. and Maud, R.R. 1994.Dispersive soils: a review from a South African perspective. *Quarterly Journal of Engineering Geology and Hydrogeology.* 27: 195-210

Bell, F.G. and Walker, D.J.H. 2000. A further examination of the nature of dispersive soils in Natal, South Africa. *Quarterly Journal of Engineering Geology and Hydrogeology.* 33: 187-199.

Berjak, M., Fincham, R., Liggitt, B. and Watson, H. 1986. Temporal and spatial dimensions of gully erosion in northern Natal, South Africa. Commission IV of the International Society for

Photogrammetry and Remote Sensing and the Remote Sensing Society. *Remote Sensing*. 26:283-293

Bernatek-Jakiel, A., Kacprzak, A. and Stolarczyk, M. 2016. Impact of soil characteristics on piping activity in a mountainous area under a temperate climate (Bieszczady Mts., Eastern Carpathians). *Catena*. 141: 117-129.

Bernatek-Jakiel, A. and Poesen, J. 2018. Subsurface erosion by soil piping: significance and research needs. *Earth Science Reviews*. 185: 1107-1128.

Boardman, J., Favis-Mortlock, D. and Foster, I. 2015. A 13-year record of erosion on badland sites in the Karoo, South Africa. *Environmental Change Institute, Oxford University Centre for the Environment.* 40:*1-43.*

Bocco, G. 1991. Gully erosion: Processes and models. Progress in Physical Geography. 15(4): 392- 406.

Botha, G. A. 1996. The geology and palaeopedology of late Quaternary colluvial sediments in northern KwaZulu-natal. Council for Geoscience, South Africa. 83: 1-165.

Bouchnak, H., Felfoul, M.S., Boussema, M.R. and Snnane, M.H. 2009. Slope and rainfall effects on the volume of sediment yield by gully erosion in the Souar lithologic formation (Tunisa). *Catena*. 78: 170-177.

Brandl, G., Cloete, M. and Anhaeusser, C.R. 2006. Sedimentary Rocks of the Karoo Supergroup. *In*: Johnson, M.R., Anhaeusser, C.R. and Thomas, R.J. (Eds). The Geology of South Africa. *Geological Society of South Africa.* 461-500.

Briassoulis, H. 2000. Analysis of Land Use Change: Theoretical and Modeling Approaches [Available online]: http://www.rri.wvu.edu/Webbook/Briassoulis/contents.htm 12/ [accessed 15 July 2021].

Calvo-Cases, A., Boix-fayos, C., Arnau-Rosalen, E. and Roxo, M.J. 2011. Gullies and rills on sodic soils. *Cuadernos de Investigación Geográfica.* 37(1): 25-40.

Capra, A., Porto, P. and Scicolone, B. 2009. Relationships between rainfall characteristics and ephemeral gully erosion in a cultivated catchment in Sicily (Italy). *Soil and Tillage Research*. 105: 77-87.

Chase, B.M. and Meadows, M.E. 2007. Late Quaternary dynamics of Southern Africa's winter rainfall zone. *Earth Science Reviews*. 84 (3-4): 103-138.

Chen, Y. and Borochovich, A. 1983. Effect of potassium on soil structure in relation to hydraulic conductivity. *Geoderma*. 30: 135-147.

Conforti, M., Aucelli P.P.C. and Robustelli, F.S. 2011. Geomorphology and GIS analysis for mapping gully erosion susceptibility in the Turbolo stream catchment (Northern Calabria, Italy). *Natural Hazards.* 56: 881-898.

Cowie, A.L., Orr, B.J., Sanchez, V.M.C., Chasek, P., Crossman, N.D., Erlewein, A., Louwagie, G., Maron, M., Metternicht, G.I., Minelli, S., Tengberg, A.E., Walter, S. and Welton, S. 2018. Land in balance: The scientific conceptual framework for Land Degradation Neutrality. *Environmental Science and Policy.* 79: 25-35

Department of Environmental Affairs. 2012. Desertification in South Africa. Available Online: [http://soer.deat.gov.za/dm_documents/World_Day_to_Combat_Desertification_ThemeArticle_17June_t1w1u.pdf]

Dube, T., Mutanga, O., Sibanda, M., Seutloali, K. and Shoko, C. 2017. Use of Landsat series data to analyse the spatial and temporal variations of land degradation in a dispersive soil environment: A case study of KinG Sabata Dalindyebo local municipality in the Eastern Cape Province, South Africa. *Physics and Chemistry of the Earth.*100:112-120.

Ellis, E. 2013. Land-use and land-cover change. [Available online]: http://www.eoearth.org/view/article/154143/ [accessed 12 May 2021

Ferrer, V., Errea, P., Alonso, E., Gomez-Gutierrez, A. and Nadal-Romero, E. 2017. A multi scale approach to assess geomorphological processes in semiarid badlands area (Ebro Depression, Spain). *Geographical Research Letters.* 43(1): 41-62.

Gallart, F., Marignani, M., Pérez-Gallego, N., Santi, E. and Maccherini, S. 2013. Thirty years of studies on badlands, from physical to vegetational approaches. A succinct review. *Catena*. 106: 4-11.

Gallart, F., Sole, A., Puigdefa bregas, J. and La zaro, R. 2002: Badland systems in the Mediterranean. *In:* Bull, L.J. and Kirkby, M.J. (Eds). Dryland rivers: hydrology and geomorphology of semi-arid channels, Chichester. *Wiley.* 299–326.

García-Ruiz, J.M., Nadal-Romero, E., Lana-Renault, N. and Beguería, S. 2013. Erosion in Mediterranean landscapes: changes and future challenges. *Geomorphology.* 198: 20-36.

Garland, G. G., Hoffman, T. and Todd, S. 2000. Soil degradation in a national review of land degradation in South Africa. [Online article].

Gholamy, A., Kreinovich, V. and Kosheleva, O. 2018. Why 70/30 or 80/20 Relation Between Training and Testing Sets: A Pedagogical Explanation*. Departmental Technical Reports (CS).* 1209.

Gillespie, W.M. 1875. A treatise on land surveying: comprising the Theory Developed from Five Elementary Principles, and the Practice with the Chain Alone, the Compass, the Transit, the Theodolite, the Plane Table, Etc. *D. Appleton & Company.* 8: 122 - 311[Digitized in 2010]

Guerschman, J.P., Paruelo, J.M., Bella, C.D., Giallorenzi, M.C. and Pacin, F. 2003. Land cover classification in the Argentine Pampas using multi-temporal Landsat TM data. *Int. J. Remote Sens.* 24: 3381–3402.

Haylock, M. and Nicholls, N. 2000. Trends in extreme rainfall indices for an updated high quality data set for Australia. *International Journal of Climatology*. 20: 1533-1541.

Han, Y., Zheng, F.L. and Xu, X.M. 2017. Effects of rainfall regime and its character indices on soil loss at loessial hillslope with ephemeral gully. *Journal of Mountain Science* 14(3): 527-538.

Jahantigh, M. and Pessarakli, M. 2011. Causes and Effects of Gully Erosion on Agricultural Lands and the Environment. *Communications in Soil Science and Plant Analysis*. 42: 2250 - 2255.

Jones, J.A.A. 2004. Soil piping and its hydrogeomorphic function. Cuaternarioy Gemorfología. 8 (3-4): 77-102.

Kakembo, V. and Rowntree, K. M. 2003. The relationship between land use and soil erosion in the communal lands near Peddie Town, Eastern Cape, South Africa. Land Degradation and Development. 14: 39-49.

Kivel, P. 1991. Urban Land Use, New York. *Longman Scientific and Technical.*

Kuhn, N. 2013. Long-term (1973-2013) vegetation change in the Groot Winterhoek Wilderness Area. (Honours thesis, Department of Biological Sciences: University of Cape Town).

Lal, R. 2001. Soil degradation by erosion. Land Degradation and Development. 12(6): 519-539.

Lambin, E. F. and Geist, H. 2006. Land-Use and Land-Cover Change: Local Processes and Global Impacts, Berlin. *Springer Verlag*.

Lambin, E. F., Geist, H. J. and Lepers, E. 2003. Dynamics of land-use and land-cover change in tropical regions. *Annual Review of Environment and Resources*. 28 (1): 205-241.

Le Roux, J. J., Newby, T. S. and Sumner, P. D. (2007). Monitoring soil erosion in South Africa at a regional scale: Review and recommendations. South African Journal of Science. 103: 329-335.

Le Roux, J.J. and Sumner, P.D. 2012. Factors controlling gully development: comparing continuous and discontinuous gullies. *Land Degradation & Development*. 23: 440-449.

Li, G.Y. and Fan, H.M. 2014. Effect of Freeze-Thaw on Water Stability of Aggregates in a Black Soil of Northeast China. *Pedosphere.* 24 (2): 285- 290.

Liberti, M., Simonielle, T., Carone, M.T., Coppola, R., D'emilio, M. and Macchiato, M. 2009. Mapping badland areas using LANDSAT TM/ETM satellite imagery and morphological data. *Geomorphology*. 106(3-4): 333-343.

Lu, D. and Weng, Q. 2005. Urban Classification Using Full Spectral Information of Landsat ETM+ Imagery in Marion County, Indiana. *Photogramm Eng Remote Sens*. 71: 1275–1284.

Mararakanye, N. and Le Roux, J.J. 2012. Gully location mapping at a national scale for South Africa. *South African Geographical Jounral.* 94(2): 208-218.

Meadows, M.E. and Hoffman, T.M. 2003. Land degradation and climate change in South Africa. *Geographical Journal*. 169(2): 168-177.

Meadows, M.E. 2003. Soil erosion in the Swartland, Western Cape Province, South Africa: implications of past and present policy and practice. Environmental Science and Policy. 6:17-28.

Montgomery, D.R. 2007. Soil erosion and agricultural sustainability. *Proceedings of the National Academy of Sciences*. 104: 13268-13272.

Moore, T. R. 1979. Rainfall erosivity in east Africa. Geographiska Annaler. 61A: 136-147.

Morgan, R. P. C. 1986. Soil erosion and conservation. Essex: Longman Group.

Nachtergaele, J. and Posen, J. 1999. Assessment of soil losses by ephemeral gully erosion using high- altitude (stereo) aerial photographs. *Earth Surface Processes and Landforms.* 24 (8): 693-706.

Nachtergaele, J., Poesen, J. and Govers, G. 2002. Ephemeral gullies. A spatial and temporal analysis of their characteristics, importance and prediction. *BELGEO*. 2: 159-182.

Nacinovic, M. G. G., Mahler, C. F. and Avelar, A. de S. 2014. Soil erosion as a function of different agricultural land use in Rio de Janeiro. The Soil and Tillage Research. 144: 164-173.

Nel, W. and Sumner, P. 2007. Intensity, energy and erosivity attributes of rainstorms in the KwaZulu-Natal Drakensberg, South Africa. *South African Journal of Science*. 103: 398 - 402.

Onwuka B. and Mang, B. 2018. Effects of soil temperature on some soil properties and plant growth. *Adv Plants Agric Res*. 8(1):34-37.

Ozsahin, E., Duru, U. and Eroglu, I. 2018. Land Use and Land Cover Changes (LULCC), a Key to Understand Soil Erosion Intensities in the Marista Basin. *Water.* 19: 335

Patton, P. C. and Schumm, S. A. 1975. Gully erosion, NW Colorado: A threshold phenomenon. Geology. 3(2): 88-99.

Perez, E. and Garcia, P. 2017. Monitoring soil erosion by raster images: from aerial photographs to drone taken pictures. *European Journal of Geography*. 8(1): 116-128.

Poesen, J., Vandekerckhove, L., Nachtergaele, J., Oostwoud, W. D., Verstraeten, G. and van Wesemael, B. 2002. Gully erosion in Dryland environments. *In Bull, L.J. Kirkby, M.J. (Ed.)*. Dryland rivers: Hydrology and geomorphology of semi-arid channels. Chichester: John Wiley and Sons. 62-229

Pontius, R.G. and Millones, M. 2011. Death to Kappa: Birth of quantity disagreement and allocation disagreement for accuracy assessment. *International Journal of Remote Sensing.* 32 (15): 4407-4429.

Ritchie, J. C. 2000. Soil erosion. Remote sensing in hydrology and water management *(Schultz GA, Engman ET ed.)*. Berlin: Springer. 1:1-102.

Roffe, SL., Fitchett, J.M. and Curtis, C.J. 2020. Determining the utility of a percentile-based wet-season start- and end-date metrics across South Africa. *Theoretical and Applied Climatology.* 140: 1331-1347.

Rosenberg, E. 2011. Land degradation. The Enviropaedia. Simonstown: Eco- Logic Publishing. [Available online]

Rowntree, K.M. 2013. The evil of sluits: a re-assessment of soil erosion in the Karoo of South Africa as portrayed in century-old sources. *Journal of Environmental Management*. 130: 98–105.

Rwanga, S.S. and Ndambuki, J.M. 2017. Accuracy Assessment of Land Use/Land Cover Classification Using Remote Sensing and GIS. *International Journal of Geosciences.* 8: 611-622.

Seutloali, K.E., Beckedahl, H.R., Dube, T. and Sibanda, M. 2015. An assessment of gully erosion along major armoured roads in south-eastern region of South Africa: a remote sensing and GIS approach. *Geocarto International.* 31(2):1-18.

Sohl, T.L and Sleeter B. M. 2012. Role of Remote Sensing for Land-Use and Land-Cover Change. *Modelling, Remote Sensing and Land Cover: Principles and Applications*. 15: 225 - 239.

Stolbovoi, V. 2002. Carbon in Russian soils. *Climatic Change*. 55 (1): 131-156.

Sumner, P. D. and Meiklejohn, I. 2000. Landscape evolution in a changing environment. *In R. Fox and K. Rowntree (Eds.)*. The geography of South Africa in a changing world. Cape Town: Oxford University Press Southern Africa. 304-325

Taruvinga, K. 2008. Gully Mapping using Remote Sensing: Case Study in KwaZulu Natal, South Africa. [Masters Thesis]. Canada; University of Waterloo.

United States Geological SurveY. 2014. *Landsat Missions*. [Available online]: http://landsat.usgs.gov/band_designations_landsat_satellites.php/ [Accessed 29 June 20121.

Valentin, C., Poesen, J. and Yong, L. 2005. Gully erosion: impacts, factors and control. Catena. 63(2-3): 132-153.

van der Eyck, J.J., MacVicar, C. N. and de Villiers, J. M. 1969. Soils of the Tugela basin - a study in sub-tropical Africa. Natal Town and Regional Planning Report. 15: 1-263

Van Dijk, A., Bruijnzeel, L. and Rosewell, C. 2002. Rainfall intensity-kinetic energy relationships: A critical literature appraisal. Journal of Hydrology. 261: 1-23.

Vanwalleghen, T., Gomez, J.A., Amate, J.I., Gonzalez de Molina, M., Vanderlinden, K., Guzman, G., Laguna, A. and Giraldez. 2017. Impact of historical land use and soil management change on soil erosion and agricultural sustainability during the Anthropocene. *Anthropocene*. 17: 13-29.

von Maltitz, G.P., Gambiza, J., Kellner, K., Rambau, T., Lindeque, L. and Kgope, B. 2019. Experiences from the South African land degradation neutrality target setting process. *Environmental Science & Policy*. 101: 54-62.

Willemen, L., Crossman, N.D., Quatrini, S., Egoh, B., Kalaba, F.K., Mbilinyi, B. and de Groot, R. 2018. Identifying ecosystem service hotspots for targeting land degradation neutrality investments in south-eastern Africa. *Journal of Arid Environments.* 159: 75-86.

Wilson, G.V., Rigby, J.R., Dabney, S.M.. 2015. Soil pipe collapses in a loess pasture of Goodwin Creek watershed. Mississippi: role of soil properties and past land use. *Earth Surf. Process*. *Landforms*. 40: 1448–1463.

Wu, Y., Ouyang, W., Hao, Z., Lin, C., Liu, H. and Wang, Y. 2018. Assessment of soil erosion characteristics in response to temperature and precipitation in a freeze-thaw watershed. *Geoderma*. 328: 56-65.

Xu, M. and Li, Q. 2016. Degradation of soil physicochemical quality by ephemeral gully erosion on sloping cropland of the hilly Loess Plateau, China. *Soil and Tillage Research*. 155: 9-18.

Yibeltal, M., Tsunekawa, A., Haregeweyn, N., Adgo, E., Meshesha, D.T., Masunaga, T., Tsubo, M., Billi, P., Ebabu K., Fenta, A.A. and Berihun, M.L. 2019. Morphological characteristics and topographic thresholds of gullies in different agro-ecological environments. *Geomorphology*. 341:15-27, Yengoh, G.T., Dent, D., Olsson, L., Tengberg, A.E. and Tucker,C.J. 2016. Use of the Normalized Difference Vegetation Index (NDVI) to Assess Land Degradation at Multiple Scales. Springer. 1:1-35.